

OPTICAL SPECTROSCOPIC OBSERVATIONS OF γ -RAY BLAZAR CANDIDATES V. TNG, KPNO AND OAN OBSERVATIONS OF BLAZAR CANDIDATES OF UNCERTAIN TYPE IN THE NORTHERN HEMISPHERE

N. ÁLVAREZ CRESPO^{1,2}, N. MASETTI³, F. RICCI⁴, M. LANDONI⁵, V. PATIÑO-ÁLVAREZ⁶, F. MASSARO^{1,2}, R. D'ABRUSCO⁷, A. PAGGI⁷, V. CHAVUSHYAN⁶, E. JIMÉNEZ-BAILÓN⁸, J. TORREALBA⁶, L. LATRONICO², F. LA FRANCA⁴, HOWARD A. SMITH⁷ & G. TOSTI⁹

version October 27, 2018: nuria

ABSTRACT

The extragalactic γ -ray sky is dominated by emission from blazars, a peculiar class of active galactic nuclei (AGNs). Many of the γ -ray sources included in *Fermi*-Large Area Telescope Third Source catalog (3FGL) are classified as a blazar candidate of uncertain type (BCU) because there is no optical spectra available in the literature to confirm their nature. In 2013 we started a spectroscopic campaign to look for the optical counterparts of the BCUs and of the Unidentified γ -ray Sources. The main goal of our investigation is to confirm the blazar nature of these sources having peculiar properties as compact radio emission and/or selected on the basis of their infrared (IR) colors. Whenever possible we also determine their redshifts. Here we present the results of the observations carried out in the Northern hemisphere in 2013 and 2014 at Telescopio Nazionale Galileo (TNG), Kitt Peak National Observatory (KPNO) and Observatorio Astronómico Nacional (OAN) in San Pedro Mártir. In this paper we describe the optical spectra of 25 sources. We confirmed that all the 15 BCUs observed in our campaign and included in our sample are blazars and we estimated the redshift for 3 of them. In addition, we present the spectra for 3 sources classified as BL Lacs in the literature but with no optical spectra available to date. We found that one of them is a quasar (QSO) at a redshift $z = 0.208$ and the other 2 are BL Lacs. Moreover, we also present 7 new spectra for known blazars listed in the Roma-BZCAT having an uncertain redshift or being classified as BL Lac candidates. We found that one of them, 5BZB J0724+2621 is a ‘changing look’ blazar. According to the spectrum available in the literature it was classified as a BL Lac but in our observation we clearly detected a broad emission line that lead to classify this source as a QSO at $z=1.17$.

Subject headings: galaxies: active - galaxies: BL Lacertae objects - radiation mechanisms: non-thermal

1. INTRODUCTION

Blazars are radio-loud active galactic nuclei (AGNs) characterised by non-thermal emission over the entire electromagnetic spectrum, from the radio band to γ rays (see e.g. Giommi et al. 2013). They show rapid variability from hours timescales in the optical band up to minutes in the γ rays (see e.g. Aharonian 2000; Homan et al. 2002), high linear polarization from the radio to the optical frequencies (see e.g. Marscher et al. 2010; Agudo et al. 2014), compact radio emission (see e.g. Taylor et al. 2007; Lister et al. 2009), flat radio spectra and superluminal motions (see e.g. Vermeulen & Cohen 1994; Kellermann et al. 2013 and references therein). The spectral energy distribution is characterised by a double bump, the first component peaking in infrared (IR)/optical wavelengths and the second one in X-rays

(for more details see e.g. Giommi & Padovani 1994, Inoue & Takahara 1996). They are strong γ -ray emitters reaching luminosities up to 10^{49} erg s^{-1} as reported in both the *Fermi*-LAT First Source Catalog (Abdo et al. 2010) and the *Fermi*-LAT Second Source Catalog (Nolan et al. 2012).

According to Stickel et al. (1991) blazars are divided into two main subclasses: BL Lac objects which present featureless optical spectra or with emission/absorption lines of rest frame equivalent width $EW < 5$ Å, and flat spectrum radio quasars that show quasar-like optical spectra with broad emission lines ($EW > 5$ Å). In the following we label the former class as BZBs and the latter as BZQ according to the nomenclature adopted in Roma-BZCAT ‘Multifrequency Catalog of BLAZARS’ (Massaro et al. 2009). In this catalogue there are listed BL Lac candidates as sources claimed to be BL Lacs in the literature but no optical spectra was found to confirm their classification. There are also sources classified as blazars of uncertain type (BZUs), adopted for sources with peculiar characteristics, similar to those previously mentioned but also showing blazar activity like occasional presence/absence of broad spectral lines, transition objects between a radio galaxy and a BL Lac or galaxies hosting a low luminosity radio nucleus. In the latest version of the Roma-BZCAT (Massaro et al. 2015a) there is one more class, BL Lacs whose optical spectra exhibit a typical elliptical galaxy spectrum with a low Ca H&K break contrast, indicated as BZGs.

With a density of the order of 0.1 sources/degree², blazars constitute the most numerous population of extragalactic γ -ray sources, about 38%. However, almost 20% of the sources above 100 MeV in the *Fermi*-LAT Third Source Catalog

¹ Dipartimento di Fisica, Università degli Studi di Torino, via Pietro Giuria 1, I-10125 Torino, Italy

² Istituto Nazionale di Fisica Nucleare, Sezione di Torino, I-10125 Torino, Italy

³ INAF - Istituto di Astrofisica Spaziale e Fisica Cosmica di Bologna, via Gobetti 101, 40129, Bologna, Italy

⁴ Dipartimento di Matematica e Fisica, Università Roma Tre, via della Vasca Navale 84, I-00146, Roma, Italy

⁵ INAF-Osservatorio Astronomico di Brera, Via Emilio Bianchi 46, I-23807 Merate, Italy

⁶ Instituto Nacional de Astrofísica, Óptica y Electrónica, Apartado Postal 51-216, 72000 Puebla, México

⁷ Harvard - Smithsonian Astrophysical Observatory, 60 Garden Street, Cambridge, MA 02138, USA

⁸ Instituto de Astronomía, Universidad Nacional Autónoma de México, Apdo. Postal 877, Ensenada, 22800 Baja California, México

⁹ Dipartimento di Fisica, Università degli Studi di Perugia, 06123 Perugia, Italy

(Abdo et al. 2014) are blazar candidates of uncertain type (BCUs). They present flat radio spectra and/or X-ray counterpart and have a multifrequency behaviour similar to blazars but there is no optical spectra to precisely allow this classification (Ackermann et al. 2012). In addition, Unidentified γ -ray Sources (UGSs) represent $\sim 33\%$ of the *Fermi*-LAT Third Source Catalog and a large fraction of these sources can be associated to blazars (Massaro et al. 2012a). Knowing how much of the emission in γ -rays comes from blazars is important to set constraints on dark matter scenarios (Mirabal et al. 2012; Berlin & Hooper 2014), to discover new classes of γ -ray emitters, to resolve the γ -ray sky and to determine the origin of the extragalactic γ -ray background (Ajello et al. 2015). For this purpose, several methods to recognise blazars as the low-energy counterparts of UGSs have been developed. For example, in the 3-dimensional IR color space generated by WISE photometry γ -ray emitting blazars lie in a region distinct from those where most of the other extragalactic sources dominated by thermal emission (Massaro et al. 2013a; D’Abrusco et al. 2014) are located. In addition, radio follow up observations of the Fermi UGSs (e.g., Kovalev 2009; Hovatta et al. 2012, 2014; Petrov et al. 2013; Schinzel et al. 2014) correlation of the peculiar IR colors with existing radio databases (Massaro et al. 2013b) and X-ray follow-up observations looking for X-ray counterparts (Paggi et al. 2013; Takeuchi et al. 2013) have been performed. Statistical studies based on γ -ray source properties have also allowed us to recognise the nature of the potential counterparts for UGSs (e.g., Ackermann et al. 2012; Mirabal et al. 2012; Hassan et al. 2013; Doert & Errando 2014). However none of these methods can be conclusive without optical spectroscopic confirmation for both BCUs and UGSs.

Since 2013 we have been carrying out a spectroscopic campaign to observe the blazar-like sources of uncertain classification as well as those selected according to the methods previously listed. In this fifth paper of the series, we present the results of optical spectroscopic observations of BCUs carried out in the Northern hemisphere at Kitt Peak National Observatory (KPNO) in Tucson (USA), Telescopio Nazionale Galileo (TNG) in La Palma (Spain) and Observatorio Astronómico Nacional (OAN) in San Pedro Mártir (Mexico) between October 2013 and July 2014. Exploratory program obtained with TNG, OAN and Multiple Mirror Telescope (MMT) were described in Paggi et al. (2014); in addition, results for observations carried out in 2013 with SOAR and KPNO were presented in Landoni et al. (2015), Massaro et al. (2015b, 2015c) and Ricci et al. (2015). In this paper we focus mainly on BCUs, although we also had the opportunity to observe Roma-BZCAT sources.

The paper is organised as follows: Section 2 contains the sample selection. We present our dataset and discuss the data reduction procedures in Section 3. Then in Section 4 we report the details on the cross-matches with multifrequency databases and catalogs of the observed targets and present the results of our analysis for different types of sources. Finally Section 5 is devoted to our summary and conclusions. We use cgs units unless otherwise stated. Spectral indices, α , are defined by flux density $S_\nu \propto \nu^{-\alpha}$. Flat spectra are defined as $\alpha < 0.5$.

2. SAMPLE SELECTION

Our final goal is to perform spectroscopic observations of a large sample of γ -ray blazar candidates selected on the basis of the IR colors (Massaro et al. 2011b) and extracted from the

WISE Blazar-like Radio-Loud Source (WIBRaLS) Catalog (D’Abrusco et al. 2014). Our observing strategy, successfully employed during the last years (see e.g. Landoni et al. 2015; Ricci et al. 2015), consists in requesting small subsamples of our main list to different telescopes to minimize the impact on their schedule. A more comprehensive presentation of our observing strategy, a detailed summary of the results of the spectroscopic observations and their interpretation will be presented in a forthcoming paper (D’Abrusco et al. 2016).

In Figure 1 we show the IR colors of the selected γ -ray blazar candidates in comparison with those of the known gamma-ray blazars associated in the 2FGL that were used to build the training sample (i.e., locus) to perform the all-sky search (see D’Abrusco et al. 2014 for more details).

The main criterion followed for the selection of the sources that we observed from the pool of potential targets has been mainly driven by the source visibility during the nights obtained at each telescope. We chose our targets considering the optimal conditions of visibility and airmass lower than 1.6. In addition interesting sources, such as blazar with uncertain redshifts and/or without an optical spectrum available in the literature have been also observed during gaps in our observing schedule. During our observing nights we also decided to re-observe sources when optimal conditions became available. For this reason, we decided to point at them because given to the optical variability of blazars there could be a chance to observe the source during a low state and thus detect emission and/or absorption features that enable a redshift measurement (Vermeulen et al. 1995; Falomo & Pian 2014).

We updated the γ -ray classification of the selected sources on the basis of the recent release of the 3FGL. Thus all our targets are now indicated as Blazar candidates of uncertain type (BCU) similar to the old class labelled as active galaxies of uncertain type (AGUs) in both the 1FGL and the 2FGL.

Our sample contains 25 sources grouped as follows:

- Fifteen sources classified as blazar candidates of uncertain type (BCU) in the 3FGL which present IR colors similar to blazars, flat radio spectrum and/or an X-ray counterpart that appear to have a multifrequency behaviour similar to blazars but there are no optical spectra to precisely allow these classifications. In particular, 12 are sources that belong to the WIBRaLS Catalog. The remaining 3 are one BZB (WISE J173605.25+203301.1), one BZQ (WISE J043307.54+322840.7) and one AGU (WISE J065340.46+281848.5), respectively, with no optical spectrum available in the literature, they are now grouped with the previous 12 since all of them are classified as BCU in the 3FGL.
- Three sources selected from the 3FGL claimed as BL Lacs in the literature but without optical spectra available to confirm it.
- Two sources that are BL Lac candidates, not necessary γ -ray emitters, classified according to the criteria of the ROMA-BZCAT (Massaro et al. 2011b).
- The remaining 5 sources are classified in the Roma-BZCAT as BZBs, but their redshifts are still uncertain.

In Table 1 we also report the 1FGL and the 2FGL names together with their old classifications and their assigned counterpart. We noticed that the latest associations for 3FGL

J0653.6+2817 and 3FGL J0433.1+3228, differ from the previous one listed in the 3FGL. However for this two cases the source pointed during our campaign is the 3FGL one as reported in Table 2. On the other hand, for 3FGL J1013.5+3440 the source was unidentified in the 2FGL catalog and we pointed the potential counterpart WISE J101349.6+344550.8 (listed in Massaro et al. 2015a) instead of the one assigned in the 3FGL.

In Table 2 we report our results and multifrequency notes for each source to verify additional information that can support the blazar-like behaviour.

3. OBSERVATIONS AND DATA REDUCTION

3.1. Kitt Peak National observatory

The spectra of twelve objects were obtained in remote observing mode at KPNO Mayall 4-m class telescope using the R-C spectrograph the nights 5th February and 4th June 2014. We adopted a slit width of $1''.2$ and a low resolution gratings (KPC10A and BL181 depending on the availability at the telescope) yielding a dispersion of 3 \AA pixel^{-1} in both cases. The average seeing during both runs was about $1''$ and conditions were clear. Wavelength calibration was accomplished using the spectra of an Helium-Neon-Argon lamp which guarantees a smooth coverage over the entire range. Due to poor long term stability during each night we needed to take into account flexures of the instruments and drift, so we took an arc frame before every target to guarantee a good wavelength solution for the scientific spectra. The accuracy reached is $\sim 3 \text{ \AA rms}$.

3.2. Telescopio Nazionale Galileo

Eight spectra were obtained using the 3.58-m Telescopio Nazionale Galileo (TNG) located at La Palma, Canary Islands (Spain). Its imaging spectrograph DOLoReS carried a 2048×2048 pixel E2V 4240 CCD; spectra were acquired with the LR-B grism and a $1''.5$ slit width which secured a nominal spectra coverage in the $3500\text{-}8200 \text{ \AA}$ range and a dispersion of $2.5 \text{ \AA pixel}^{-1}$. The TNG data were acquired between October 2013 and July 2014. We adopted the same data reduction procedure for TNG as for KPNO observations. Wavelength calibration was achieved with the spectra of an Helium-Neon lamp acquired between 2 exposures of a same object.

3.3. Observatorio Astronómico Nacional San Pedro Mártir

Five objects were observed with the 2.1 m telescope of the Observatorio Astronómico Nacional (OAN) in San Pedro Mártir (Mexico) on September and October 2014. The telescope carries a Boller & Chivens spectrograph and a 1024×1024 pixel E2V-4240 CCD. The slit width was $2''.5$. The spectrograph was tuned in the $\sim 4000 - 8000 \text{ \AA}$ range with a resolution of $10 \text{ \AA pixel}^{-1}$. Wavelength calibration was done using the spectra of a cooper-Helium-Neon-Argon lamp.

The data reduction has been performed according to our standard procedures. Further details are given in Masetti et al. (2013), Ricci et al. (2015) and Massaro et al. (2015c).

The set of spectroscopic data acquired was optimally extracted and reduced following standard procedures with IRAF (Horne 1986; Tody 1986). For each acquisition we performed bias subtraction, flat field correction and cosmic rays rejection. To remove cosmic rays we achieved 2 or 3 individual exposures for each target and averaged them according to their signal to noise ratios. We then exploited the availability of

the two individual exposures in the case of dubious detected spectral features to better reject spurious ones.

We dereddened the spectra for the galactic absorption assuming E_{B-V} values taken by Schlegel et al. (1998) relation. Although our program did not require precise photometric calibration, we observed a spectrophotometric standard star to perform relative flux calibration on each spectrum. The overall spectral shape is correct, but the absolute calibration may suffer from sky condition issues, such seeing and transparency. To detect faint spectral features, especially because our targets might be BL Lac objects, aimed at estimating redshifts, we also present normalised spectra.

4. RESULTS

Here we report all the results of our optical analysis for the selected sources divided in four groups. We have searched for additional multifrequency information that can support the blazar-like nature in radio, IR, optical and X-ray surveys and in both NASA Extragalactic Database (NED) and SIMBAD Astronomical Database. All the selected sources with their corresponding multifrequency notes are listed in Table 2. There is also a note in cases where the spectral energy distribution (SED) of the source is presented in Takeuchi et al. (2013) and if the radio counterpart has a flat radio spectrum (marked as ‘rf’). The surveys and catalogs used to search for the counterparts of our targets are listed in Table 3. Note that we use the same symbol for the X-ray catalogs of *XMM-Newton* *Chandra* and *Swift* because these X-ray observatories perform only pointed observations. There is the possibility that the pointed observation related to the field of the *Fermi* source was not requested as follow up but for another reason. Therefore, the discovery of the X-ray counterpart for an associated and/or identified source could be serendipitous.

4.1. Gamma-ray Active Galaxies of Uncertain type

Details of the 15 BCUs observed in our sample are listed below. Multifrequency notes relative to each source are reported in Table 2. The spectra of the whole sample are shown in the Figures 3 to 25 together with their finding charts. Our spectroscopic observations allow us to confirm that all these sources are BL Lac objects and we have been able to determine the redshift in one case in which the BL Lac shows absorption features from the host elliptical galaxy. For another source we could fix a lower redshift limit due to the presence of an intervening system seen along the line of sight.

The spectra of WISE J014935.28+860115.4 associated with 3FGL J0145.6+8600 is dominated by the emission of the host elliptical galaxy rather than by non-thermal continuum arising from the jet, the features distinguished are: G band, doublet Ca H+K ($EW_{obs} = 0.4 - 0.7 \text{ \AA}$) and Mg I ($EW_{obs} = 0.6 \text{ \AA}$). These features enable us to estimate a redshift of $z = 0.15$ (see Figure 4). In the case of the optical counterpart WISE J065344.26+281547.5 associated with 3FGL J0653.6+2817 the presence of an intervening doublet system of Mg II ($EW_{obs} = 1.3 - 1.0 \text{ \AA}$) allows us to set a lower limit on its redshift of $z > 0.45$ (see Figure 6). The spectra of WISE J164734.91+495000.5, counterpart of 3FGL J1647.4+4950 shows a broad emission line that we tentatively identify with $H\alpha$ ($EW_{obs} = 27.7$). On the basis of our optical spectra and the radio data we classify the source as a FSRQ at a redshift $z=0.049$ (see Figure 13). This redshift is consistent with the previous value published by Falco et al. (1998) where the spectrum is described. In the rest of the BCUs only

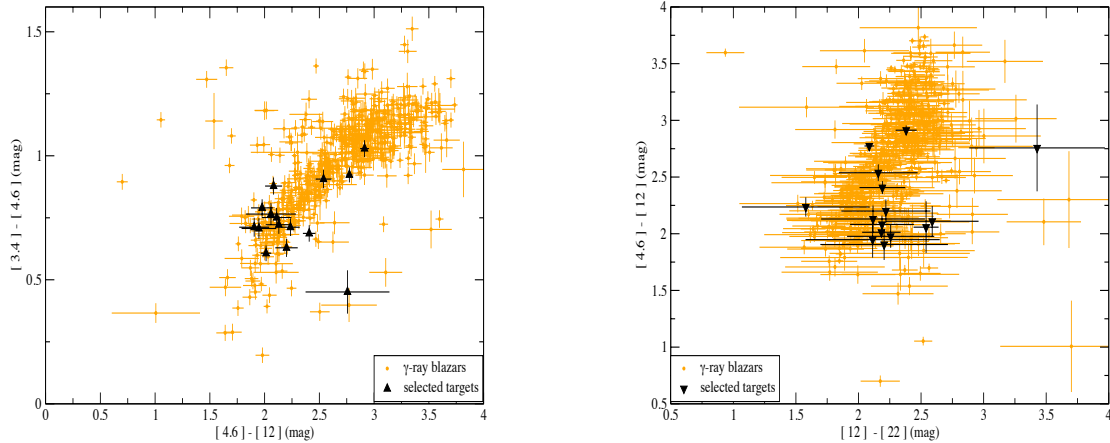


FIG. 1.— In orange the gamma-ray blazars from the WIBRaLS catalog that define the so called *locus* (i.e., the 3-dimensional region of the IR colors parameter space occupied by the associated gamma-ray blazars in the 2FGL with a WISE counterpart, see D’Abrusco et al. 2014 for additional details). *Left*: Projection of the selected targets in the *WISE* gamma-ray strip in the [3.4] - [4.6] versus [4.6] - [12] color-color plane. *Right*: Projection of the selected targets in the [4.6] - [12] versus [12] - [22] color-color plane.

featureless continuum spectra are shown so we can conclude they are BL Lacs but we did not fix any redshift (Figures 9 to 16).

4.2. *Fermi* BL Lacs with no optical spectra

During our northern campaign we have observed 3 sources claimed in the literature as BL Lacs but with no optical spectra available at the time of the observation. For the optical counterparts of the sources 3FGL J0103.4+5336 and 3FGL J2021.9+0630 we were able to confirm the BL Lac nature but not to estimate the redshift because in neither our spectra are there features present (see Figures 17 and 19 respectively). On the basis of our optical spectra we classify the counterpart of 3FGL J1013.5+3440 as a QSO at a redshift $z = 0.208$, this was possible due to the identification of the lines [O II] ($EW_{obs} = 17.2\text{\AA}$), [Ne III] ($EW_{obs} = 4.1\text{\AA}$), $H\beta$ ($EW_{obs} = 4.5\text{\AA}$), the doublet [O III] ($EW_{obs} = 14.3 - 15.8\text{\AA}$) and $H\alpha$ ($EW_{obs} = 48.5\text{\AA}$) (see Figure 18). This is consistent with a BZQ classification but the lack of radio data did not permit us to verify the flatness of the radio spectrum as expected for BZQs.

4.3. BL Lac candidates in the Roma-BZCAT

Here we discuss the BZB candidates in the Roma-BZCAT in our observed sample. Table 2 reports the Roma-BZCAT name, that on the *Fermi* counterpart when associated with a γ -ray source in the 3FGL. The spectra of this sample are shown in Figures 20 and 21 together with their finding charts. We classify 5BZB J0724+2621 as a QSO, not as a BZQ again because of the lack of radio data. It shows a broad emission line ($EW_{obs} = 26.8\text{\AA}$) that we tentatively identify as Mg II, yielding a redshift estimate of $z = 1.17$ (see Figure 20). The other source 5BZB J0814-1012 (a.k.a 3FGL J0814.1-1012) shows a featureless continuum which allow us to confirm its classification as a BL Lac (see Figure 21).

4.4. Roma-BZCAT sources with uncertain nature or unknown redshifts

In this subsample of 5 sources we confirmed the BL Lac nature for all of them but, unfortunately, it was not possible to establish their redshifts. In particular we re-observed 5BZB J0333+2916 (a.k.a 3FGL J0333.6+2916) and confirm its BL Lac nature but not the lower limit of the redshift set before as $z > 0.14$ in Shaw et al. (2013a), because our observations show only a featureless continuum (see Figure 22). The same situation occurs for 5BZB J0942-0759 (a.k.a 3FGL J0942.1-0756), the spectra is dominated by a featureless continuum and it is not possible to determine the redshift ($z > 0.46$ in Shaw et al. 2013a, see Figure 23). In the case of the source 5BZG J1414+3430 we have not been able to confirm the previous redshift value of $z = 0.275$ in White et al. (2000) (see Figure 24). For the source 5BZB J2036+6553 (a.k.a 3FGL J2036.4+6551) we do not see any features on top of the non-thermal continuum and the confirmation of $z > 0.30$ given in Shaw et al. (2013a) was not possible (see Figure 25). Finally for the last source 5BZB J2323+4210 (a.k.a 3FGL J2323.9+4211) the spectra is featureless so it was not possible to confirm the value $z=0.059$ given by Padovani et al. (1995). A featureless spectra of this source was presented also by Shaw et al. (2013a) and by Massaro et al. (2015c) (see Figure 26).

5. SUMMARY AND CONCLUSIONS

We present the results of our 2013 and 2014 optical spectroscopic campaign in the Northern hemisphere with the Telescopio Nazionale Galileo (TNG), Kitt Peak National Observatory (KPNO) and Observatorio Astronómico Nacional (OAN) in San Pedro Mártir. The main goal of our program is to use optical spectroscopy to confirm the nature of sources selected among the BCUs for having low radio frequency spectra (i.e. below ~ 1 GHz) or peculiar IR colours.

Confirmation of blazar nature among these objects will improve and refine future associations for the *Fermi* catalog.

Also, once our campaign is completed, this will yield to understand the efficiency and completeness of the association method based on IR colours. One more aim is to search for redshift estimates of the potential UGS counterparts.

During our campaign we also observed several active galaxies of uncertain type as defined according to the *Fermi* catalogs (Ackerman et al. 2011a; Nolan et al. 2012; Abdo et al. 2014) to verify if they are blazars. In addition we observed several sources that already belong to the Roma-BZCAT because either there were no optical spectra available in the literature, or their estimated redshifts were still uncertain when the catalog was released.

The total number of targets presented is 25. The results of this part of the spectroscopic campaign can be reported as follows:

- In the BCU subsample, all of the sources have a blazar nature. One of them, namely WISE J014935.28+860115.4 is dominated by absorption of the host galaxy, and were able to detect absorption lines in the optical spectrum leading to a redshift measurement of $z = 0.15$. We have also been able to set a lower limit for WISE J065344.26+281547.5 of 0.45 thanks to the detection of a Mg II intervening system.
- We obtained the spectra of 3 sources classified as BL Lacs in the literature but with no spectra published at the time of the observations. We found that 2 of them are indeed BL Lacs but the optical spectrum of WISE J101336.51+344003.6 shows this source is a QSO at $z = 0.208$.
- For the 5 BZBs listed in the Roma-BZCAT with uncertain redshift estimation we were not able to obtain any z value with our observations.
- We also analysed 2 BL Lac candidates listed in the Roma-BZCAT. According to our results 5BZB J0814-1012 is confirmed as a BZB. The spectra of the source 5BZB J0724+2621 observed by White et al. (2000) showed a featureless continuum corresponding to the classification as a BL Lac, but in our observations we detected a broad emission line. This strongly indicates that the source was previously observed during a state dominated by non-thermal radiation that did not allow to detect emission lines. During our observation we observed this previously classified BL Lac showing a broad emission line that led to a QSO classification.

It is a ‘changing look’ blazar (see e.g. Giommi et al. 2012). and we classify it as a QSO at a redshift $z = 1.17$. It has been suggested that this transition could happen due to a change in the bulk Lorentz factor of the jet (Bianchin et al. 2009). Other interpretation is that these blazars are instead FSRQs, whose emission lines are swamped by the relativistically boosted jet flux (Ghisellini et al. 2012).

We thank the anonymous referee for useful comments that led to improvements in the paper. We are grateful to Dr. D. Hammer and Dr. W. Boschin for their help to schedule, prepare and perform the KPNO and the TNG observations, respectively. We thank E. Cavazzuti for her help checking tables. This investigation is supported by the NASA grants NNX12AO97G and NNX13AP20G. H. A. Smith acknowledges partial support from NASA/JPL grant RSA 1369566.

The work by G. Tosti is supported by the ASI/INAF contract I/005/12/0. V.C. and J.T. are supported by the CONACyT research grant 151494 (Mexico). Part of this work is based on archival data, software or on-line services provided by the ASI Science Data Center. This research has made use of data obtained from the high-energy Astrophysics Science Archive Research Center (HEASARC) provided by NASA’s Goddard Space Flight Center; the SIMBAD database operated at CDS, Strasbourg, France; the NASA/IPAC Extragalactic Database (NED) operated by the Jet Propulsion Laboratory, California Institute of Technology, under contract with the National Aeronautics and Space Administration. Part of this work is based on the NVSS (NRAO VLA Sky Survey): The National Radio Astronomy Observatory is operated by Associated Universities, Inc., under contract with the National Science Foundation and on the VLA low-frequency Sky Survey (VLSS). The Molonglo Observatory site manager, Duncan Campbell-Wilson, and the staff, Jeff Webb, Michael White and John Barry, are responsible for the smooth operation of Molonglo Observatory Synthesis Telescope (MOST) and the day-to-day observing programme of SUMSS. The SUMSS survey is dedicated to Michael Large whose expertise and vision made the project possible. The MOST is operated by the School of Physics with the support of the Australian Research Council and the Science Foundation for Physics within the University of Sydney. This publication makes use of data products from the Wide-field Infrared Survey Explorer, which is a joint project of the University of California, Los Angeles, and the Jet Propulsion Laboratory/California Institute of Technology, funded by the National Aeronautics and Space Administration. This publication makes use of data products from the Two Micron All Sky Survey, which is a joint project of the University of Massachusetts and the Infrared Processing and Analysis Center/California Institute of Technology, funded by the National Aeronautics and Space Administration and the National Science Foundation. This research has made use of the USNOFS Image and Catalogue Archive operated by the United States Naval Observatory, Flagstaff Station (<http://www.nofs.navy.mil/data/fchpix/>). Funding for the SDSS and SDSS-II has been provided by the Alfred P. Sloan Foundation, the Participating Institutions, the National Science Foundation, the U.S. Department of Energy, the National Aeronautics and Space Administration, the Japanese Monbukagakusho, the Max Planck Society, and the Higher Education Funding Council for England. The SDSS Web Site is <http://www.sdss.org/>. The SDSS is managed by the Astrophysical Research Consortium for the Participating Institutions. The Participating Institutions are the American Museum of Natural History, Astrophysical Institute Potsdam, University of Basel, University of Cambridge, Case Western Reserve University, University of Chicago, Drexel University, Fermi lab, the Institute for Advanced Study, the Japan Participation Group, Johns Hopkins University, the Joint Institute for Nuclear Astrophysics, the Kavli Institute for Particle Astrophysics and Cosmology, the Korean Scientist Group, the Chinese Academy of Sciences (LAMOST), Los Alamos National Laboratory, the Max-Planck-Institute for Astronomy (MPIA), the Max-Planck-Institute for Astrophysics (MPA), New Mexico State University, Ohio State University, University of Pittsburgh, University of Portsmouth, Princeton University, the United States Naval Observatory, and the University of Washington. The WENSS project was a collaboration between the Netherlands Foundation for Research in Astronomy and the Leiden Observatory. We acknowledge the

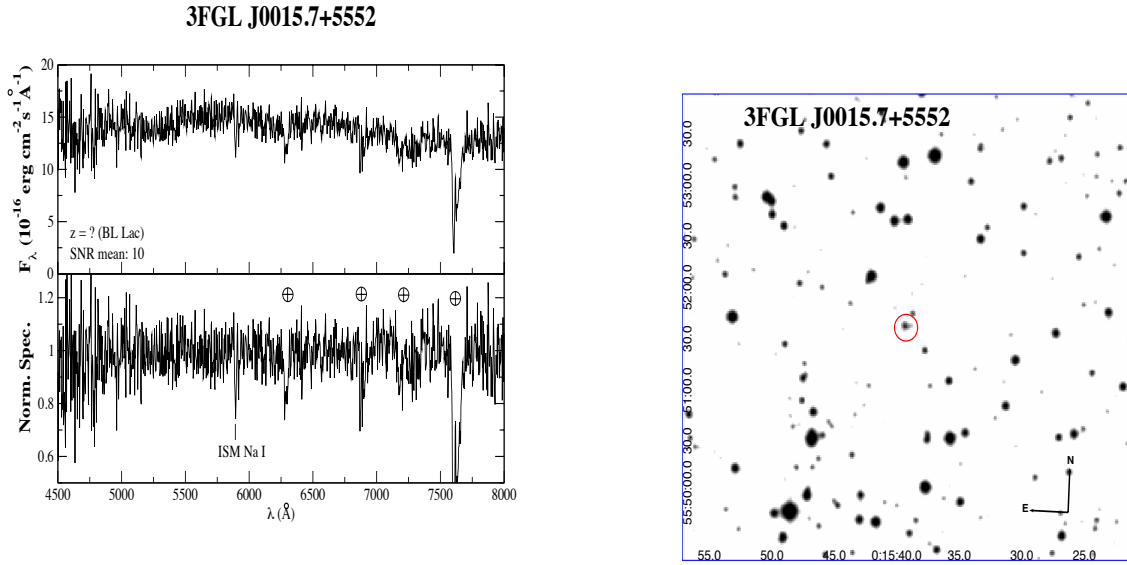


FIG. 2.— *Left*: Upper panel) The optical spectra of WISE J001540.13+555144.7, potential counterpart of 3FGL J0015.7+5552. It is classified as a BL Lac on the basis of its featureless continuum. The average signal-to-noise ratio (SNR) is also indicated in the figure. Lower panel) The normalized spectrum is shown here. Telluric lines are indicated with a symbol. *Right* The $5' \times 5'$ finding chart from the Digital Sky Survey (red filter). The potential counterpart of 3FGL J0015.7+5552 pointed during our observations is indicated by the red circle.

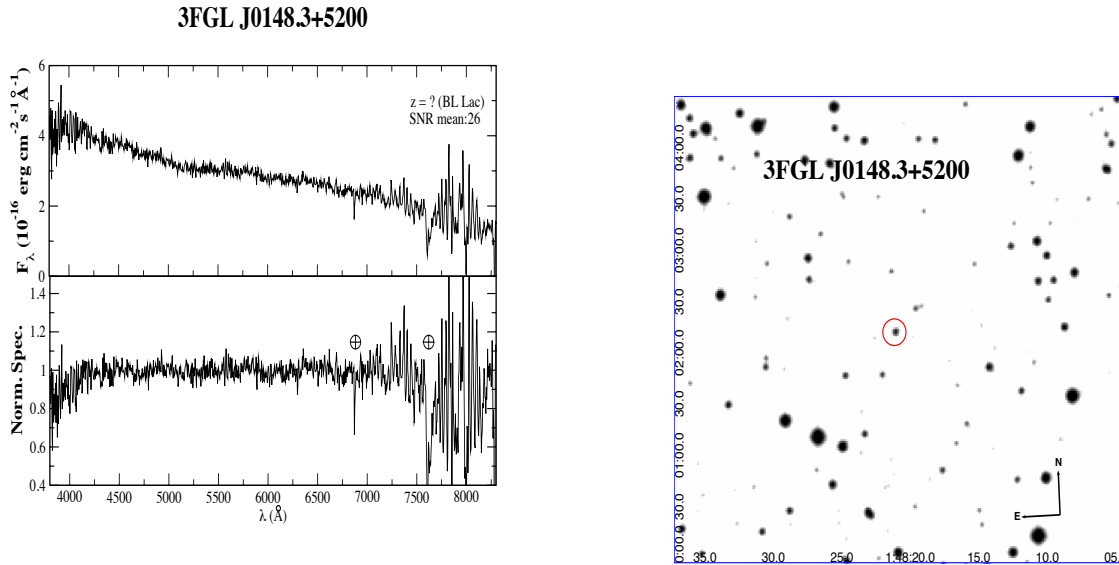


FIG. 3.— *Left*: Upper panel) The optical spectra of WISE J014820.33+520204.9, potential counterpart of 3FGL J0148.3+5200. It is classified as a BL Lac on the basis of its featureless continuum. The average signal-to-noise ratio (SNR) is also indicated in the figure. Lower panel) The normalized spectrum is shown here. *Right*: The $5' \times 5'$ finding chart from the Digitized Sky Survey (red filter) as in Fig. 2.

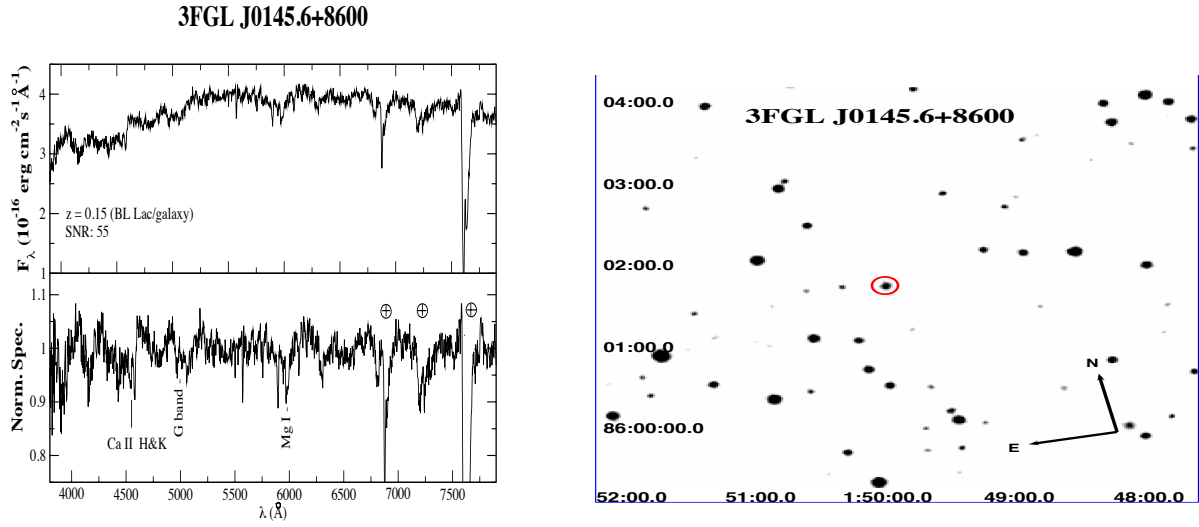


FIG. 4.— *Left*: Upper panel) The optical spectra of WISE J014935.28+860115.4, potential counterpart of 3FGL J0145.6+8600. The spectrum is dominated by the emission of the host elliptical galaxy and shows G band, doublet Ca H+K ($\lambda_{obs} = 4518 - 4578\text{\AA}$) and Mg I ($\lambda_{obs} = 6028\text{\AA}$). These features enable us to measure a redshift of $z=0.15$. SNR is also indicated in the figure. Lower panel) The normalized spectrum is shown here. *Right*: The $5' \times 5'$ finding chart.

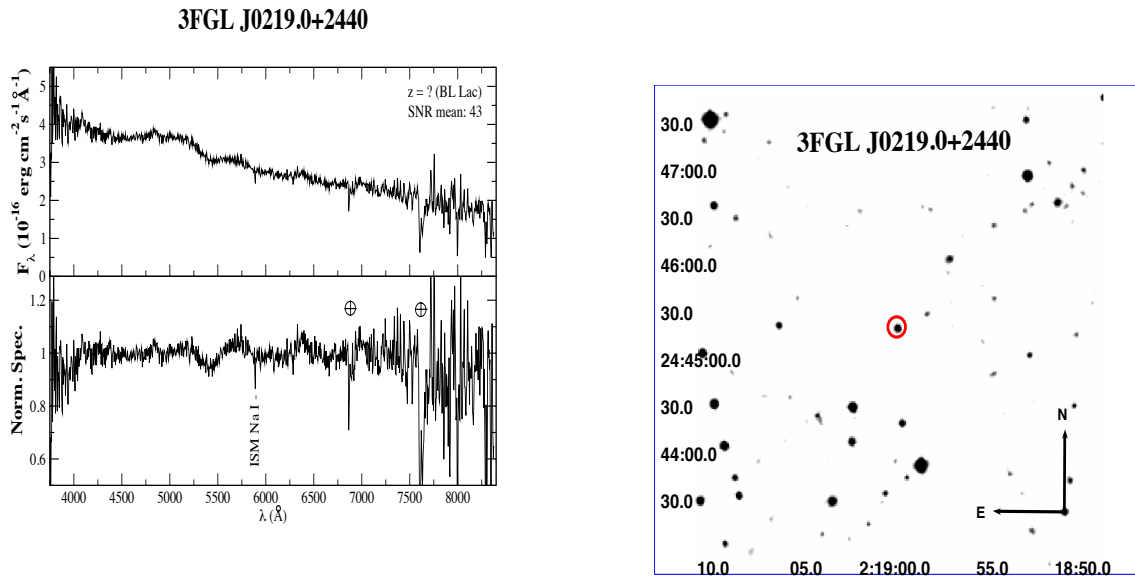


FIG. 5.— *Left*: Upper panel) The optical spectra of WISE J021911.90+244052.6, potential counterpart of 3FGL J0219.0+2440. It is classified as a BL Lac on the basis of its featureless continuum. SNR is also indicated in the figure. Lower panel) The normalized spectrum is shown here. *Right*: The $5' \times 5'$ finding chart.

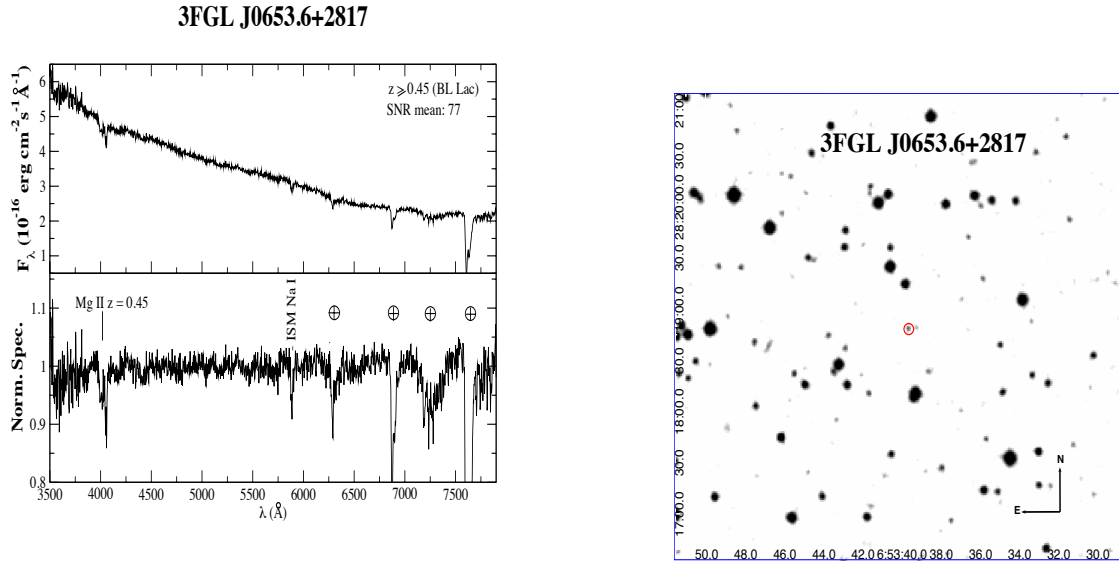


FIG. 6.— *Left*: Upper panel) The optical spectra of WISE J065344.26+281547.5, potential counterpart of 3FGL J0653.6+2817. Our observation shows presence of an intervening doublet system of Mg II ($\lambda_{obs} = 4018 - 4055\text{\AA}$) with a lower redshift limit of $z > 0.45$. SNR also indicated in the figure. Lower panel) The normalized spectrum is shown here. *Right*: The $5' \times 5'$ finding chart.

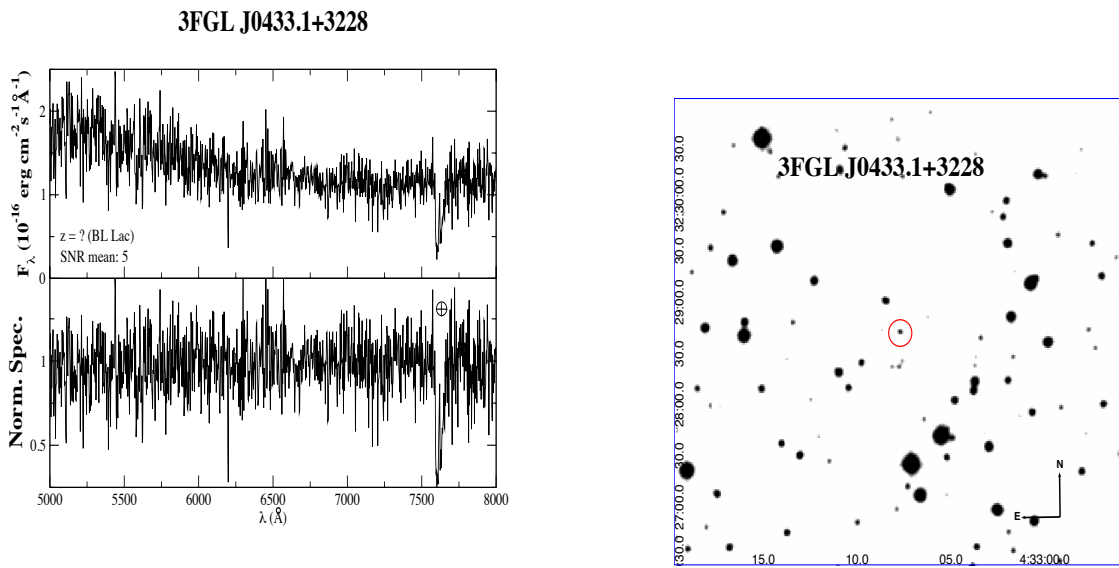


FIG. 7.— *Left*: Upper panel) The optical spectra of WISE J043307.54+322840.7, potential counterpart of 3FGL J0433.1+3228. It is classified as a BL Lac on the basis of its featureless continuum. SNR also indicated. Lower panel) The normalized spectrum is shown here. *Right*: The $5' \times 5'$ finding chart.

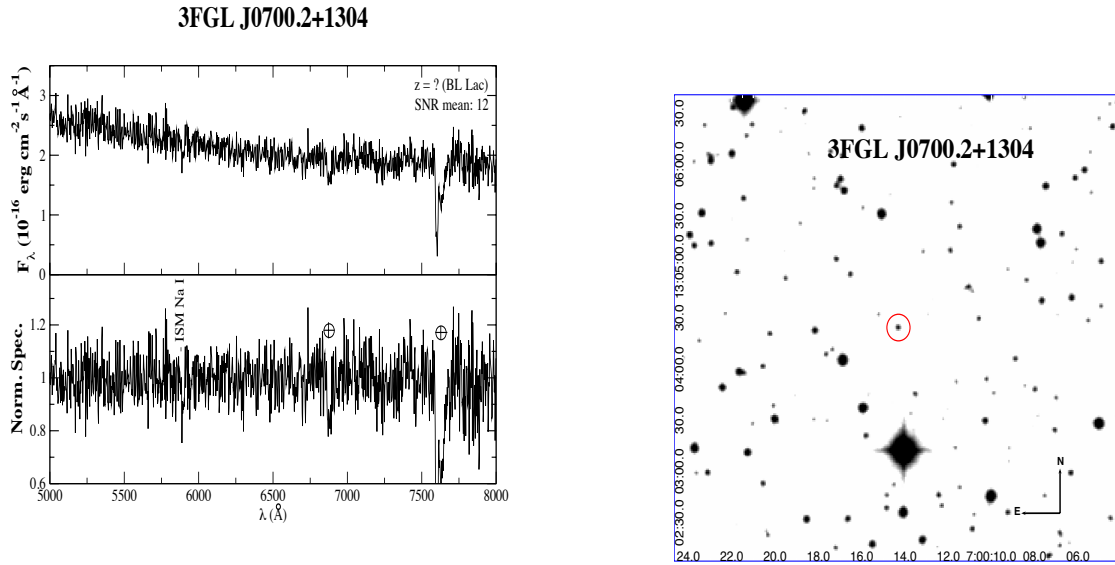


FIG. 8.— *Left*: Upper panel) The optical spectra of WISE J070014.31+130424.4, potential counterpart of 3FGL J0700.2+1304. It is classified as a BL Lac on the basis of its featureless continuum. SNR is also indicated in the figure. Lower panel) The normalized spectrum is shown here. *Right*: The $5' \times 5'$ finding chart.

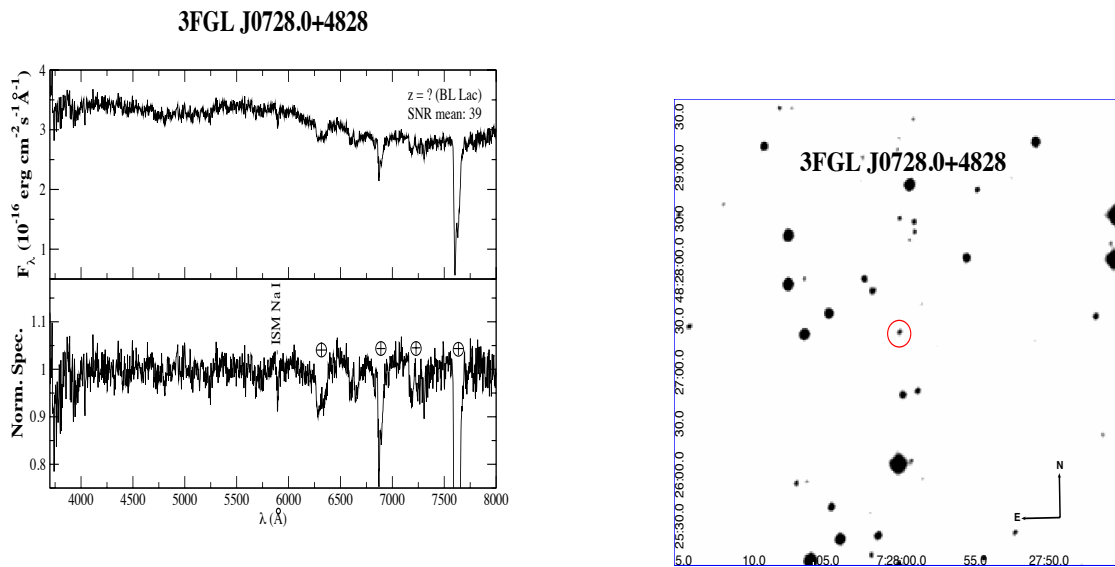


FIG. 9.— *Left*: Upper panel) The optical spectra of WISE J072759.84+482720.3, potential counterpart of 3FGL J0728.0+4828. It is classified as a BL Lac on the basis of its featureless continuum. SNR also indicated in the figure. Lower panel) The normalized spectrum is shown here. *Right*: The $5' \times 5'$ finding chart.

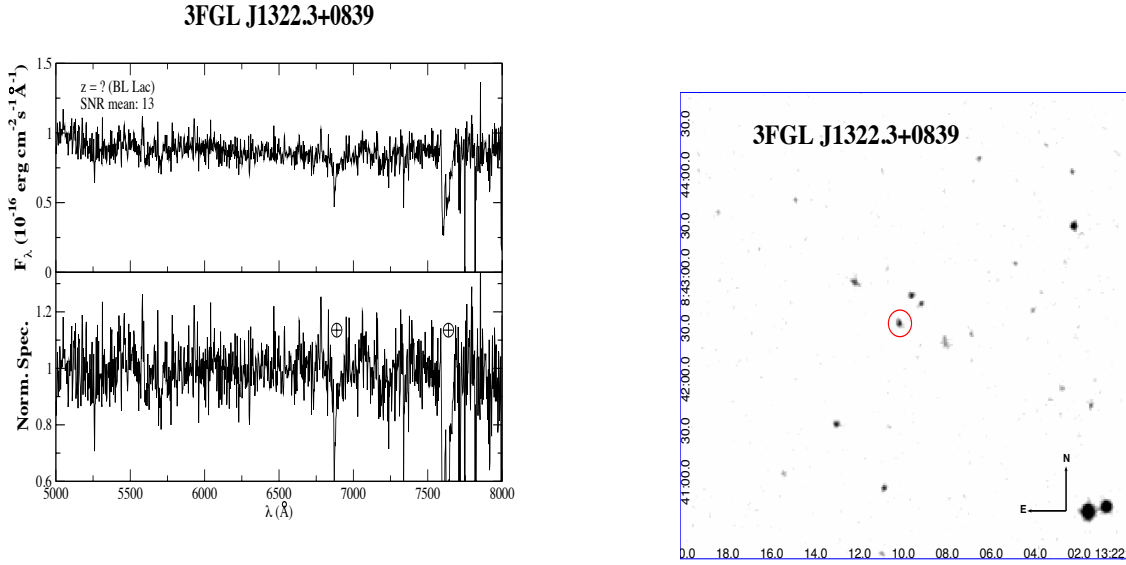


FIG. 10.— *Left*: Upper panel) The optical spectra of WISE J132210.17+084232.9, potential counterpart of 3FGL J1322.3+0839. It is classified as a BL Lac on the basis of its featureless continuum. SNR is also indicated in the figure. Lower panel) The normalized spectrum is shown here. *Right*: The $5' \times 5'$ finding chart.

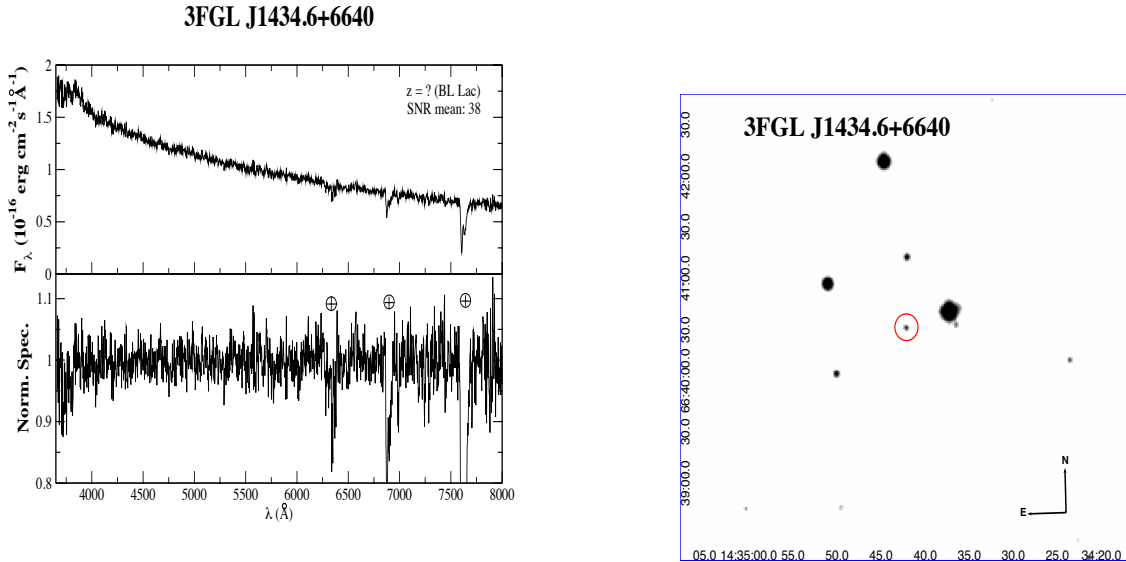
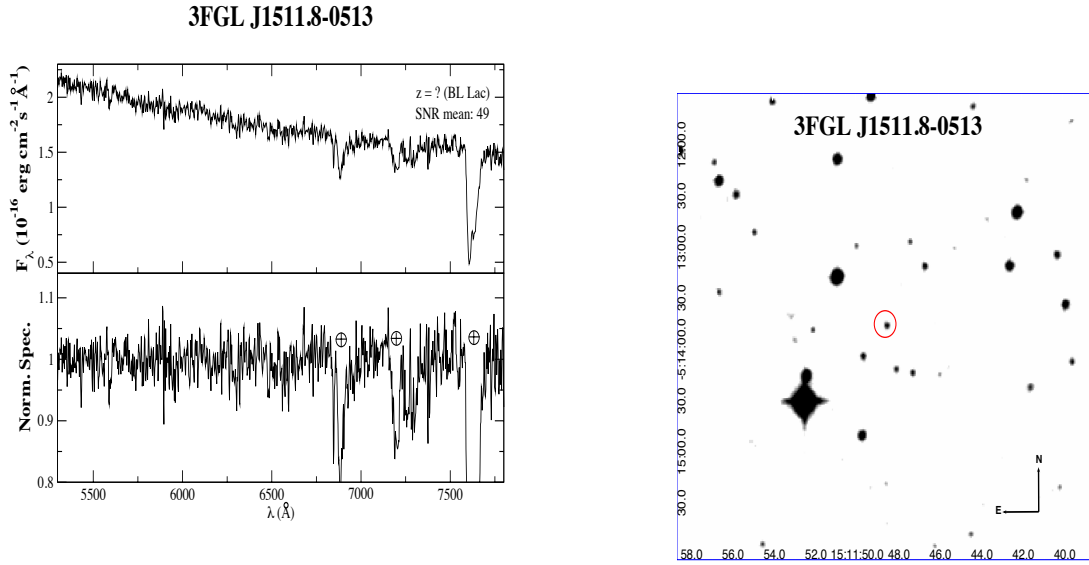


FIG. 11.— *Left*: Upper panel) The optical spectra of WISE J143441.46+664026.5, potential counterpart of 3FGL J1434.6+6640. It is classified as a BL Lac on the basis of its featureless continuum. The average signal-to-noise ratio (SNR) is also indicated in the figure. Lower panel) The normalized spectrum is shown here. *Right*: The $5' \times 5'$ finding chart.



s

FIG. 12.— *Left:* Upper panel) The optical spectra of WISE J151148.56-051346.9, potential counterpart of 3FGL J1511.8-0513. It is classified as a BL Lac on the basis of its featureless continuum. SNR is also indicated in the figure. Lower panel) The normalized spectrum is shown here. *Right:* The $5' \times 5'$ finding chart.

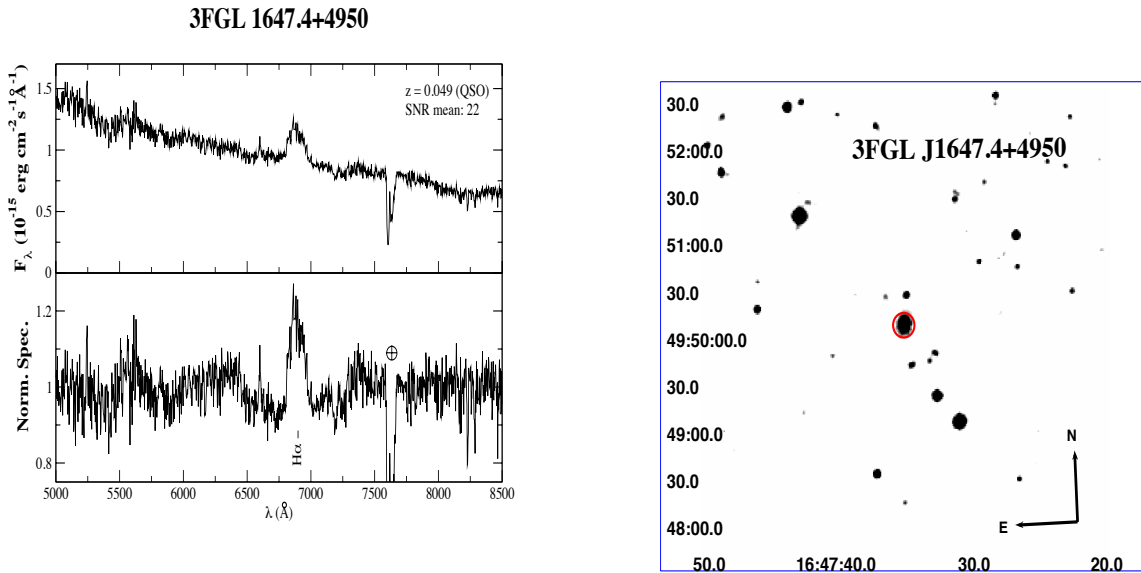


FIG. 13.— *Left:* Upper panel) The optical spectra of WISE J164734.91+495000.5, potential counterpart of 3FGL J1647.4+4950. Our observation shows an emission line of $H\alpha$ ($\lambda_{obs} = 6887\text{\AA}$). The source is a FSRQ at $z=0.049$. SNR is also indicated in the figure. Lower panel) The normalized spectrum is shown here. *Right:* The $5' \times 5'$ finding chart.

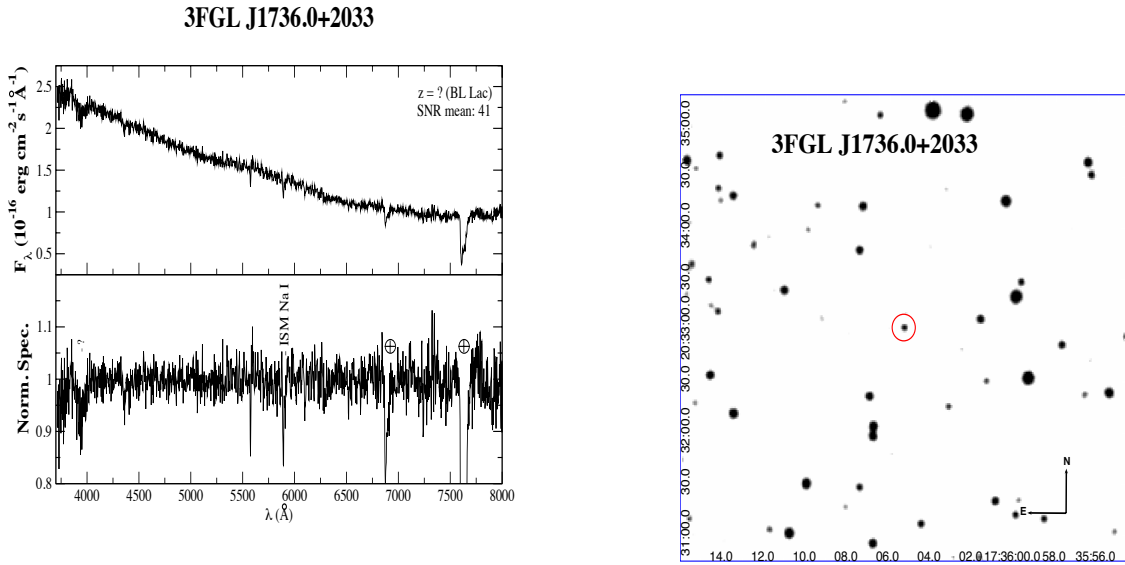


FIG. 14.— *Left:* Upper panel) The optical spectra of WISE J173605.25+203301.1, potential counterpart of 3FGL J1736.0+2033. It is classified as a BL Lac on the basis of its featureless continuum. SNR is also indicated in the figure. Lower panel) The normalized spectrum is shown here. *Right:* The 5' x 5' finding chart.

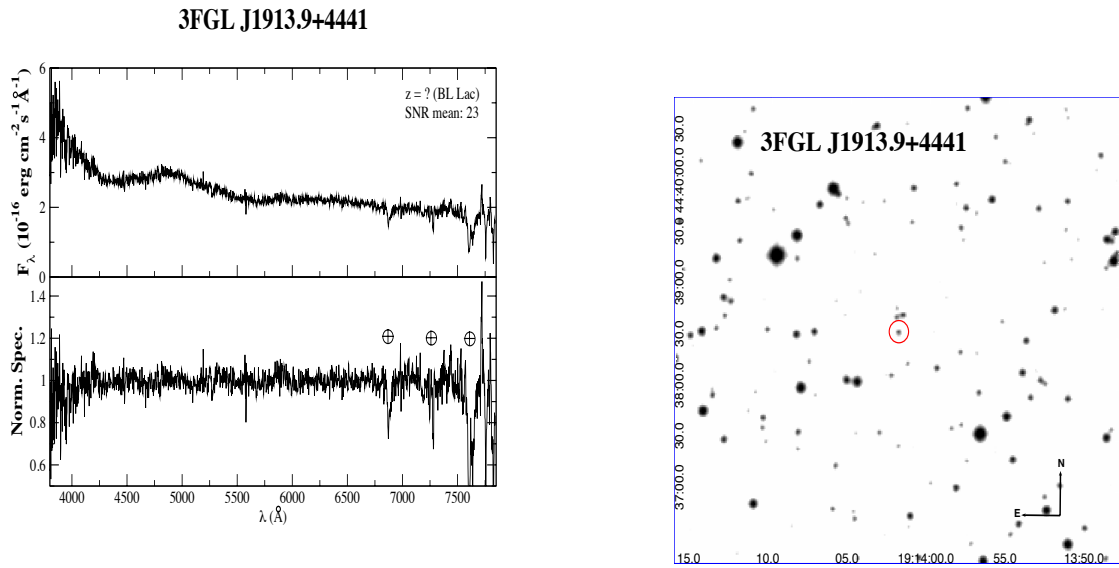


FIG. 15.— *Left:* Upper panel) The optical spectra of WISE J191401.88+443832.2, potential counterpart of 3FGL J1913.9+4441. It is classified as a BL Lac on the basis of its featureless continuum. SNR is also indicated in the figure. Lower panel) The normalized spectrum is shown here. *Right:* The 5' x 5' finding chart.

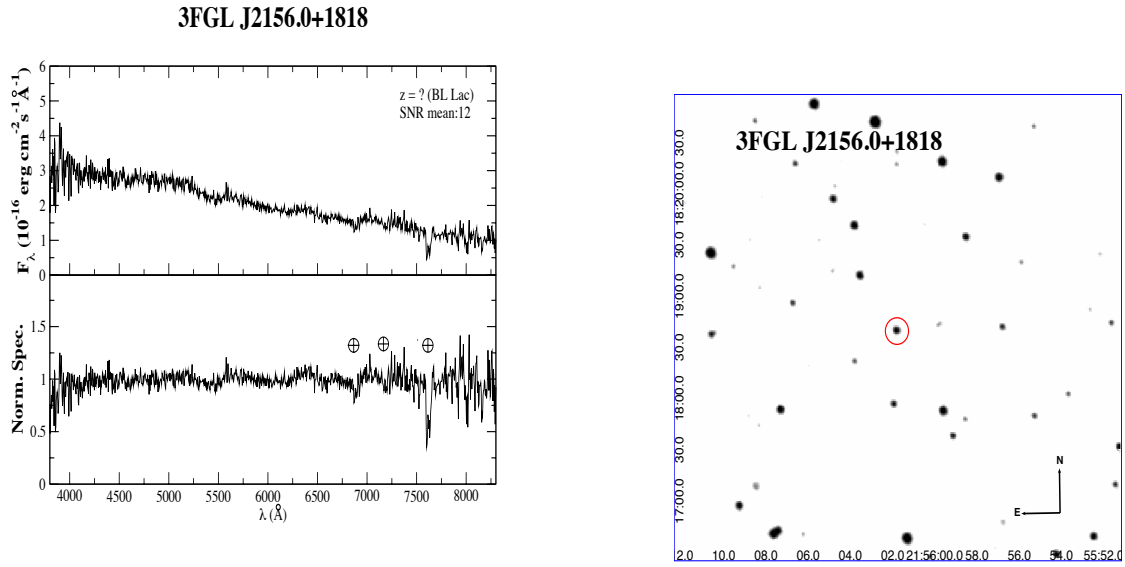


FIG. 16.— *Left*: Upper panel) The optical spectra of WISE J215601.64+181837.1, potential counterpart of 3FGL J2156.0+1818. It is classified as a BL Lac on the basis of its featureless continuum. The average signal-to-noise ratio (SNR) is also indicated in the figure. Lower panel) The normalized spectrum is shown here. *Right*: The $5' \times 5'$ finding chart.

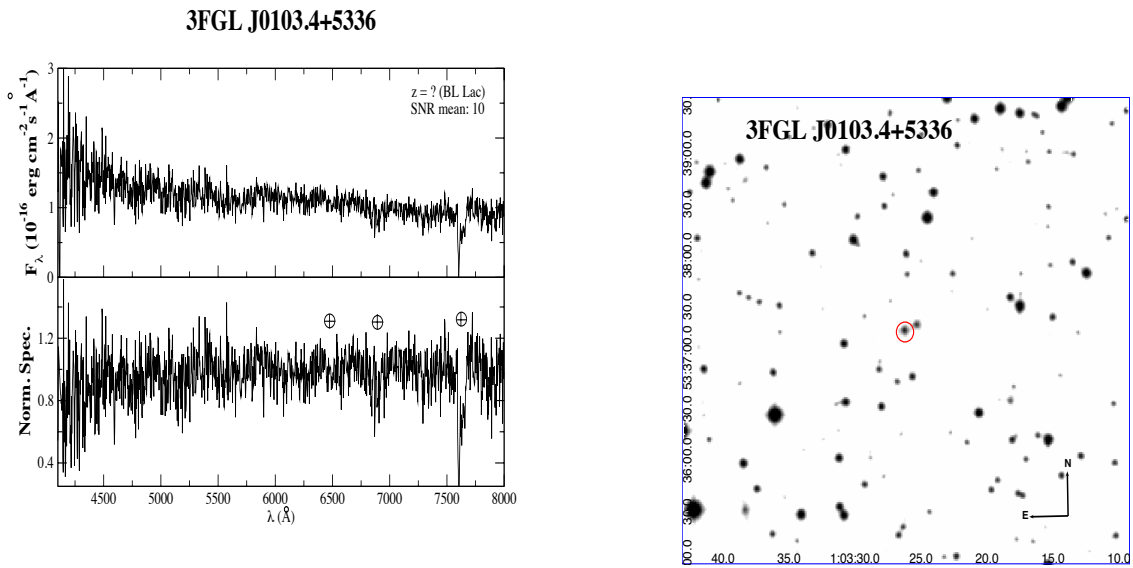


FIG. 17.— *Left*: Upper panel) The optical spectra of WISE J010325.89+533713.4, potential counterpart of 3FGL J0103.4+5336. It is classified as a BL Lac on the basis of its featureless continuum. SNR is also indicated in the figure. Lower panel) The normalized spectrum is shown here. *Right*: The $5' \times 5'$ finding chart.

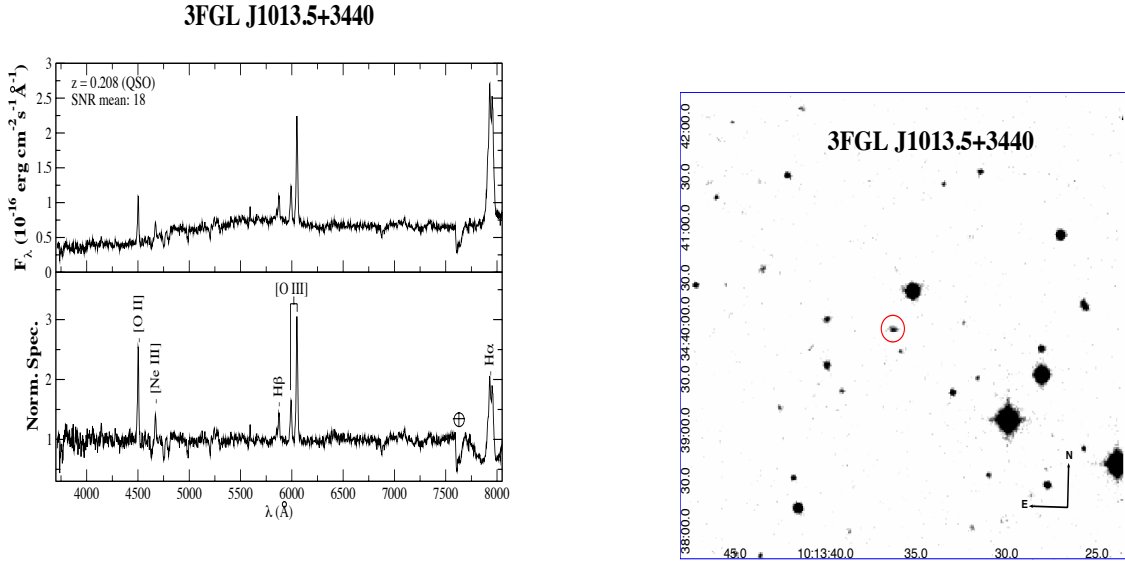


FIG. 18.— *Left:* Upper panel) The optical spectra of WISE J101336.51+344003.6, potential counterpart of 3FGL J1013.5+3440. It is classified as a QSO at $z = 0.208$. Identification of the lines [O II] ($\lambda_{obs} = 4502\text{\AA}$), [Ne III] ($\lambda_{obs} = 4671\text{\AA}$), $H\beta$ ($\lambda_{obs} = 5874\text{\AA}$), the doublet [O III] ($\lambda_{obs} = 5992 - 6050\text{\AA}$) and $H\alpha$ ($\lambda_{obs} = 7939\text{\AA}$). SNR is also indicated in the figure. Lower panel) The normalized spectrum is shown here. *Right:* The $5' \times 5'$ finding chart.

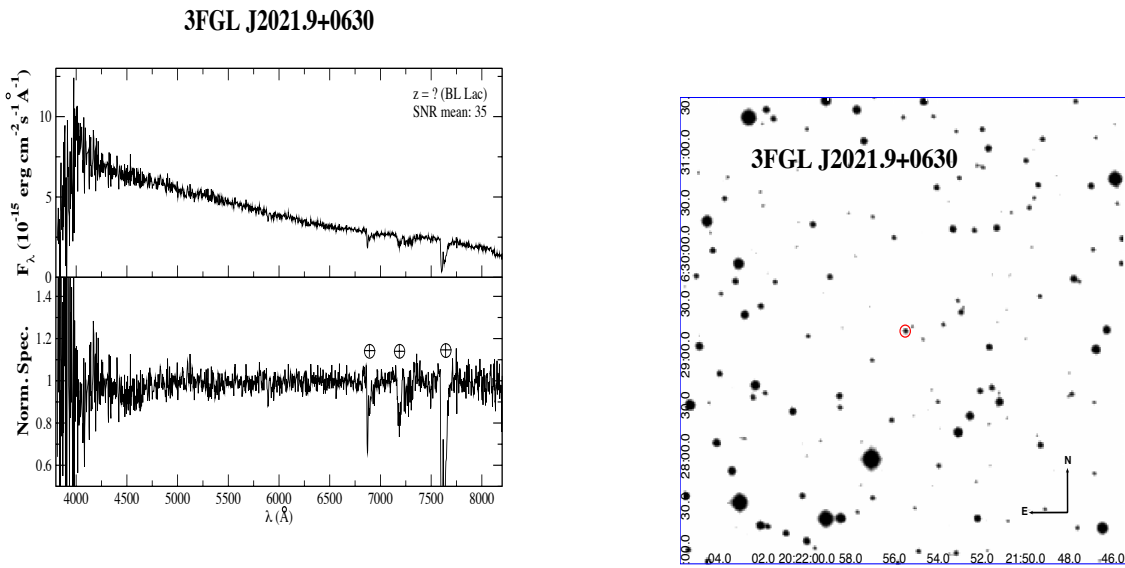


FIG. 19.— *Left:* Upper panel) The optical spectra of WISE J202155.45+062913.6 potential counterpart of 3FGL J2021.9+0630. It is classified as a BL Lac on the basis of its featureless continuum. SNR is also indicated in the figure. Lower panel) The normalized spectrum is shown here. *Right:* The $5' \times 5'$ finding chart.

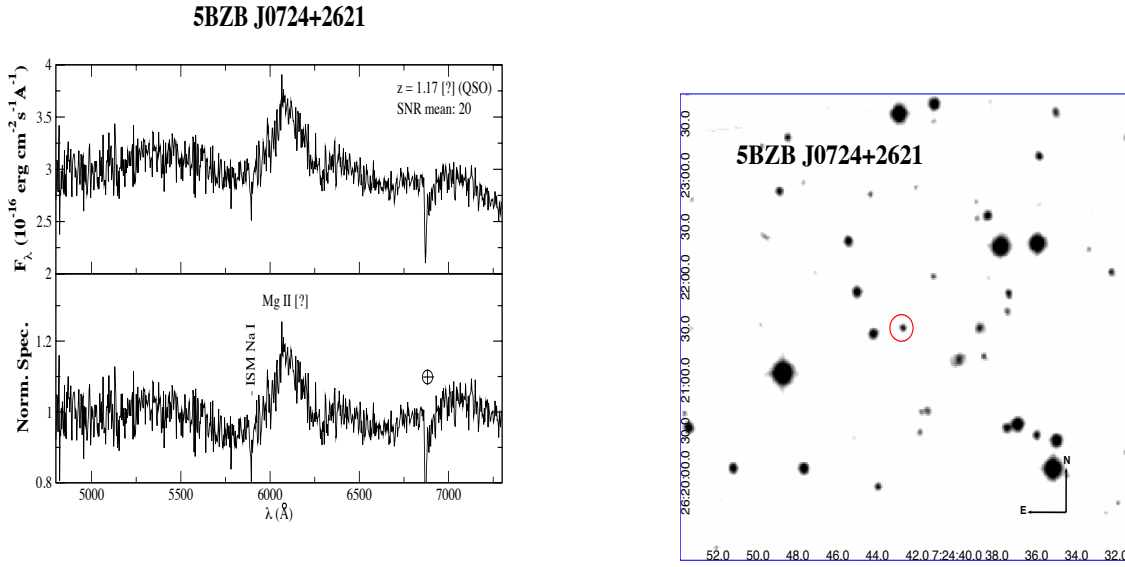


FIG. 20.— *Left:* Upper panel) The optical spectra of 5BZBJ0724+262 listed in the Roma-BZCAT. It is classified as a QSO at $z = 1.17$. Broad emission line Mg ($\lambda_{obs} = 6099\text{\AA}$). SNR is also indicated in the figure. Lower panel) The normalized spectrum is shown here. *Right:* The $5' \times 5'$ finding chart.

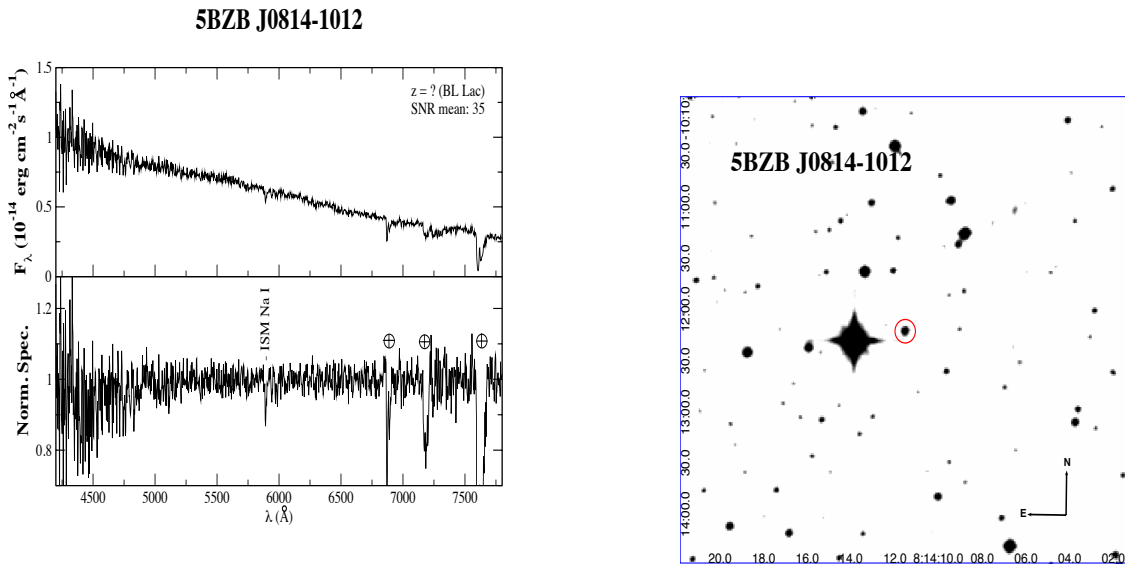


FIG. 21.— *Left:* Upper panel) The optical spectra of 5BZBJ0814-1012 listed in the Roma-BZCAT potential counterpart of 3FGL J0814.1-1012. It is classified as a BZB on the basis of its featureless continuum. SNR is also indicated in the figure. Lower panel) The normalized spectrum is shown here. *Right:* The $5' \times 5'$ finding chart.

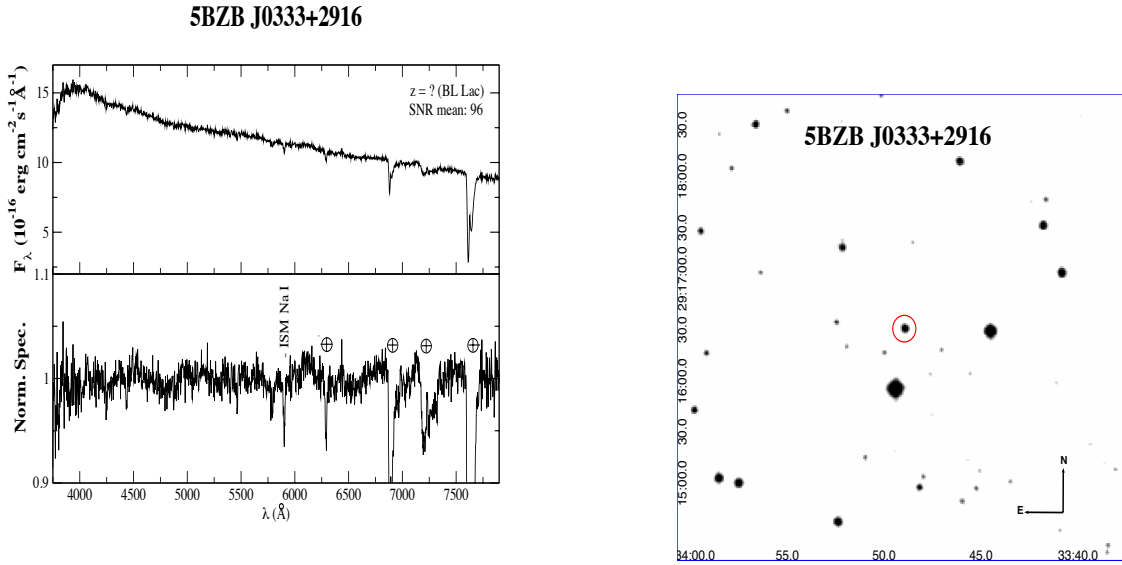


FIG. 22.— *Left:* Upper panel) The optical spectra of 5BZB J0333+2916 listed in the Roma-BZCAT potential counterpart of 3FGL J0333.6+2916. It is classified as a BZB on the basis of its featureless continuum. SNR is also indicated in the figure. Lower panel) The normalized spectrum is shown here. *Right:* The 5' x 5' finding chart.

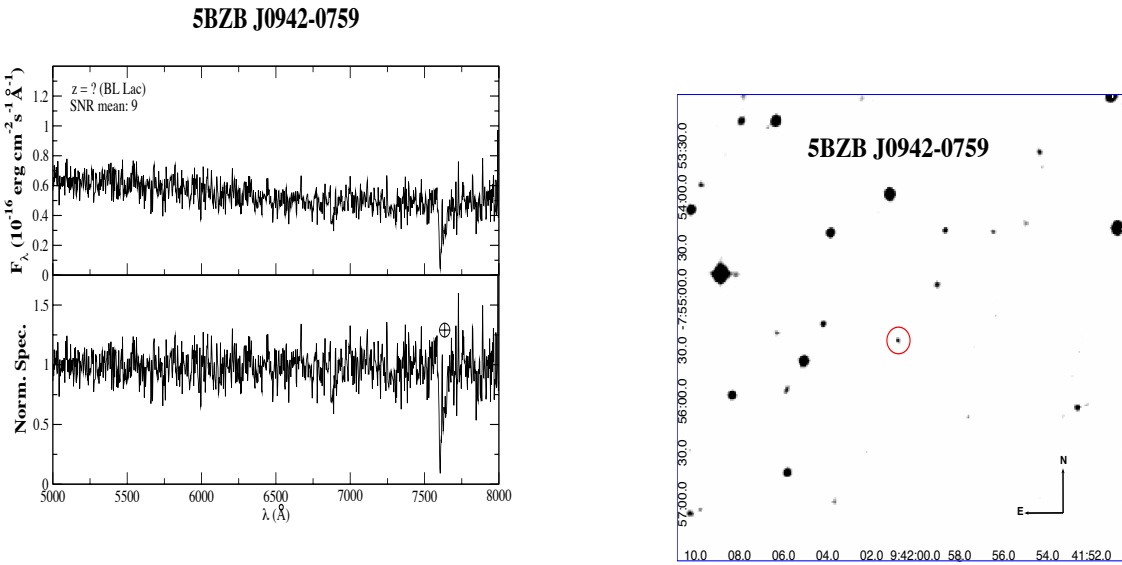


FIG. 23.— *Left:* Upper panel) The optical spectra of 5BZB J0942-0759 listed in the Roma-BZCAT potential counterpart of 3FGL J0942.1-0756. It is classified as a BZB on the basis of its featureless continuum. SNR is also indicated in the figure. Lower panel) The normalized spectrum is shown here. *Right:* The 5' x 5' finding chart.

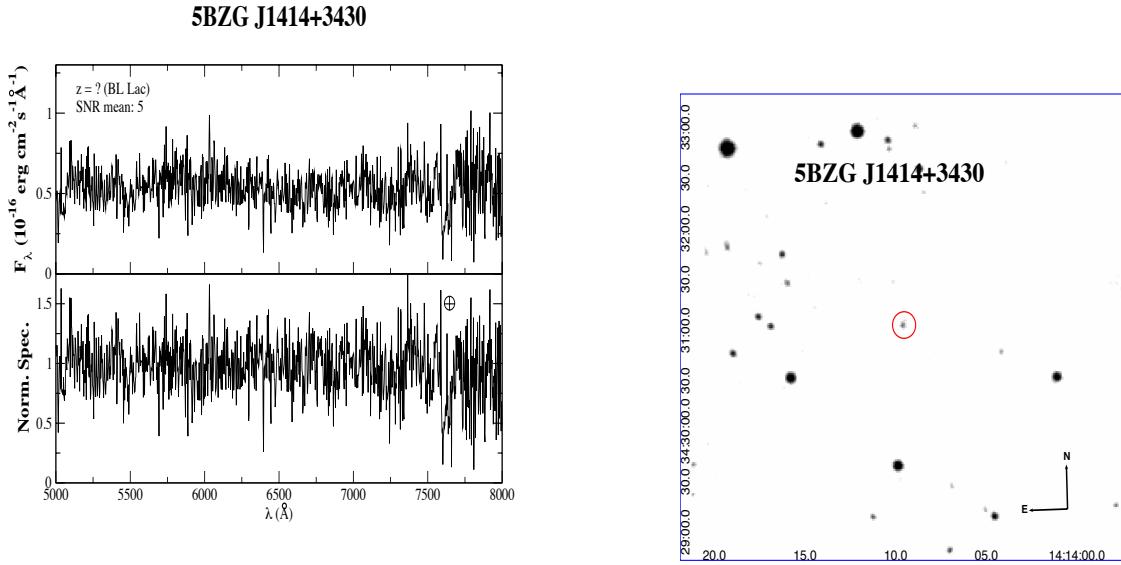


FIG. 24.— *Left:* Upper panel) The optical spectra of 5BZG J1414+3430 listed in the Roma-BZCAT. It is classified as a BZB on the basis of its featureless continuum. SNR is also indicated in the figure. Lower panel) The normalized spectrum is shown here. *Right:* The 5' x 5' finding chart.

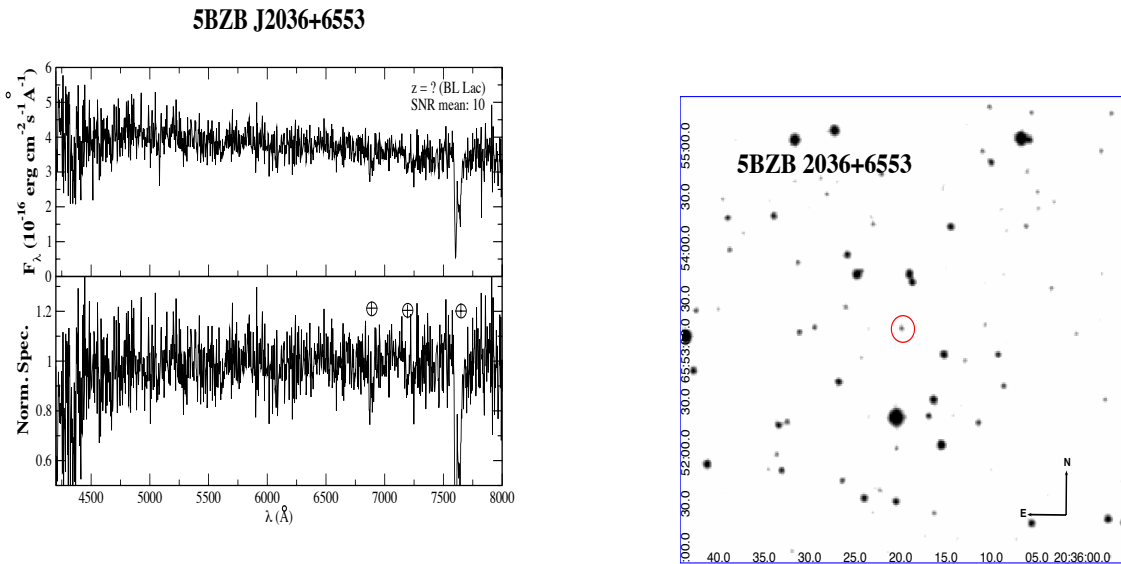


FIG. 25.— *Left:* Upper panel) The optical spectra of 5BZB J2036+6553 listed in the Roma-BZCAT potential counterpart of 3FGL J2036.4+6551. It is classified as a BZB on the basis of its featureless continuum. SNR is also indicated in the figure. Lower panel) The normalized spectrum is shown here. *Right:* The 5' x 5' finding chart.

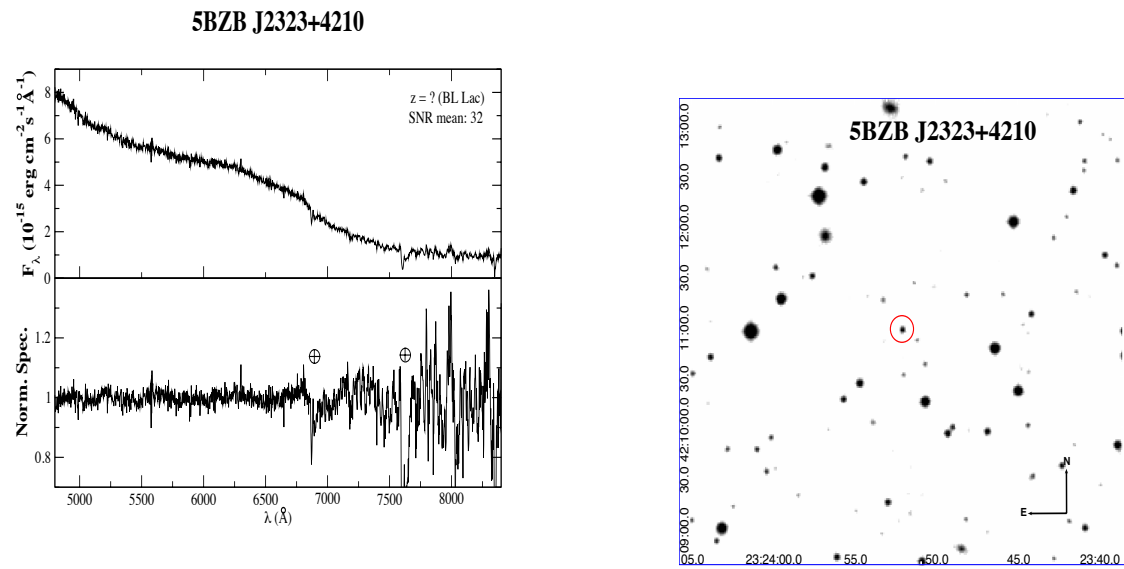


FIG. 26.— *Left:* Upper panel) The optical spectra of 5BZB J2323+4210 listed in the Roma-BZCAT potential counterpart of 3FGL J2323.9+4211. It is classified as a BZB on the basis of its featureless continuum. SNR is also indicated in the figure. Lower panel) The normalized spectrum is shown here. *Right:* The $5' \times 5'$ finding chart.

TABLE 3

LIST OF CATALOGS IN WHICH WE SEARCHED FOR ADDITIONAL MULTIFREQUENCY INFORMATION.

Survey/Catalog name	Acronym
Allen et al. (2006) A Low-Frequency Sky Survey Discrete Source Catalog	VLSS
Becker et al. (2005) Westerbork Northern Sky Survey	WENSS
Becker et al. (2005) Parkes-MIT-NRAO Surveys	PMN
Becker et al. (2005) Texas Survey of Radio Sources	TEXAS
Becker et al. (2005) Low-frequency Radio Catalog of Flat-spectrum Sources	LORCAT
Becker et al. (2005) NRAO VLA Sky Survey	NVSS
Becker et al. (2005) A Faint Images of The Radio Sky at Twenty-Centimeter	FIRST
Becker et al. (2005) Green Bank catalog of radio sources	87 GB
Becker et al. (2005) Green Bank 6-cm Radio Source Catalog	GB6
Becker et al. (2005) WISE all-sky survey in the Allwise Source catalog	WISE
Becker et al. (2005) Two Micron All Sky Survey	2MASS
Becker et al. (2005) Sloan Digital Sky Survey Data Release 9	SDSS DR9
Becker et al. (2005) 6-degree-Field Galaxy Redshift Survey	6dFGS
Becker et al. (2005) ROSAT Bright Source Catalog	RBSC
Becker et al. (2005) ROSAT Faint Source Catalogs	RFSC
Becker et al. (2005) <i>MM-Newton</i> Slew Survey	XMMSL
Becker et al. (2005) Deep Swift X-Ray Telescope Point Source Catalog	1XSPS
Becker et al. (2005) <i>Chandra</i> Source Catalog	CSC

Column description. (1): Survey/Catalog name, (2): Acronym, (3): Reference, (4): Symbol used in multifrequency notes in Table 2.

TABLE 2

FERMI SOURCES CLASSIFIED AS ACTIVE GALAXIES OF UNCERTAIN TYPE ACCORDING TO THE 3LAC; 2) FERMI SOURCES CLASSIFIED AS BL LACS IN THE 3LAC; 3) FERMI SOURCES CLASSIFIED AS BL LAC CANDIDATES, BOTH DETECTED AND NOT DETECTED BY FERMI FOR WHICH NO OPTICAL SPECTROSCOPIC INFORMATION WERE FOUND IN THE LITERATURE OR BZBS WITH UNCERTAIN/UNKNOWN REDSHIFT ESTIMATE.

3FGL name	Alternative name	R. A. (J2000)	Dec. (J2000)	Telescope	Obs. Date (yyyy-mm-dd)	Exp. (sec)	SNR	multifrequency notes*	z	class
-----------	------------------	---------------	--------------	-----------	------------------------	------------	-----	-----------------------	---	-------

Fermi Active Galaxies of Uncertain type

J0015-7-5552	WISE J001540.13+555144.7	00:15:40.1	+55:51:44	KPNO	2014-02-05	2x1200	10	N, 87, GB, rf, w, M, X, x	?	BL Lac
J0148-3-5200	WISE J014820.33+520204.9	01:48:20.2	+52:02:06	OAN	2014-10-01	3x1800	26	L, N, 87, GB, rf, w	?	BL Lac
J0145-6-8600	WISE J014935.28+860115.4	01:49:29.8	+86:01:14	TNG	2013-10-12	2x1200	55	W, N, w	0.15	BL Lac/galaxy
J0219-0-2440	WISE J021900.40+244520.6	02:19:00.4	+24:45:20	OAN	2014-10-02	3x1800	43	N, w	?	BL Lac
J0433-1-3228	WISE J043307.54+322840.7	04:33:07.7	+32:28:40	KPNO	2014-02-05	2x600	5	N, 87, GB, w, rf	?	BL Lac
J0653-6-2817	WISE J065340.46+281848.5	06:53:40.2	+28:18:49	TNG	2014-03-26	2x1200	77	N, w	> 0.45	BL Lac
J0700-2-1304	WISE J070014.31+130424.4	07:00:14.3	+13:04:24	KPNO	2014-02-05	2x1350	12	N, w	?	BL Lac
J0728-0-4828	WISE J072759.84+482720.3	07:27:59.9	+48:27:20	TNG	2014-05-07	2x1200	39	L, N, 87, GB, w	?	BL Lac
J1322-3-0839	WISE J132210.17+084033.9	13:22:10.2	+08:40:33	KPNO	2014-02-05	2x1350	13	N, w, s, g	?	BL Lac
J1434-6-6640	WISE J143441.46+664026.5	14:34:41.8	+66:40:27	TNG	2014-03-26	2x1200	38	N, w, X	?	BL Lac
J1511-8-0513	WISE J151148.56+051346.9	15:11:48.6	-05:13:45	TNG	2014-07-02	2x1200	49	N, w, SED in Takeuchi+13	?	BL Lac
J1647-4-4950	WISE J164734.91+495000.5	16:47:34.9	+49:50:00	KPNO	2014-06-05	2x300	22	N, 87, GB, c, rf, w, M, s, g, X, (z = 0.047 Falco+98)	0.049	OSO
J1736-0-2033	WISE J173605.25+203301.1	17:36:05.3	+20:33:01	TNG	2014-05-31	2x1200	41	N, w, U, g, X	?	BL Lac
J1913-9-4441	WISE J191401.88+443832.2	19:14:01.9	+44:38:33	OAN	2014-09-30	3x1800	23	N, w	?	BL Lac
J2156-0-1818	WISE J215601.64+181837.1	21:56:01.6	+18:18:39	OAN	2014-10-02	3x1800	12	N, U, g, X	?	BL Lac

Fermi BL Lacs with no optical spectra

J0103-4-5336	WISE J010325.89+533713.4	01:03:25.9	+53:37:13	KPNO	2014-02-05	2x600	10	N, 87, w, rf, X	?	BL Lac
J1013-5-3440	WISE J101336.51+344003.6	10:13:36.0	+34:40:06	TNG	2014-03-26	2x1200	18	N, w, X	0.208	OSO
J2021-9-0630	WISE J202155.45+062913.6	20:21:55.5	+06:29:14	KPNO	2014-02-05	2x1200	35	Pm, N, 87, w	?	BL Lac

BZB candidates in the Roma-BZCAT

J0814-1-1012	5BZBJ0724+2621	07:24:42.7	+26:21:31	KPNO	2014-02-05	2x1800	20	N, w, M, (White+2000)	1.17	OSO
	5BZBJ0814+1012	08:14:11.7	-10:12:10	KPNO	2014-02-05	2x1200	35	N, A, w, 6	?	BL Lac

BZBs listed in the Roma-BZCAT with uncertain z

J0333-6-2916	5BZB J0333+2916	03:33:49.0	+29:16:31	TNG	2013-10-12	2x1200	96	T, N, 87, GB, rf, U, X, (z > 0.14 Shaw+13)	?	BL Lac
J0942-1-0756	5BZB J0942-0759	09:42:00.6	-07:55:17	KPNO	2014-02-05	2x1350	9	N, w, (z > 0.46 Shaw+13)	?	BL Lac
J2036-4+6551	5BZG J1414+3430	14:14:09.3	+34:30:57	KPNO	2014-02-05	2x600	5	N, F, w, M, s, X, (z = 0.275 Bauer+00)	?	BL Lac
J2323-9+4211	5BZB J2036+6553	20:36:19.9	+65:53:14	KPNO	2014-02-05	2x3000	10	N, 87, w, (z > 0.3 Shaw+13)	?	BL Lac
	5BZB J2323+4210	23:23:52.1	+42:10:58	OAN	2014-10-25	3x1800	32	N, w, M, X, (z = 0.059 Padovani+95, Shaw+13, Massaro+15c)	?	BL Lac

Column description. (1): 3FGL name, (2): Alternative name, (3): Right Ascension (Equinox J2000), (4): Declination (Equinox J2000), (5): Telescope: Kitt Peak National observatory (KPNO); Telescopio Nazionale Galileo (TNG); Observatorio Astronómico Nacional San Pedro Mártir (OAN), (6): Observation Date, (7): Exposure time, (8): Signal to Noise Ratio, (9): multifrequency notes (see Table 3), (10):

REFERENCES

- Abdo, A. A., Ackermann, M., Ajello, M. et al. 2010 *ApJS*, 188, 405
- Abdo A. A., et al., 2014, submitted
- Ackermann, M., Ajello, M., Allafort, A. et al. 2011a *ApJ*, 743, 171
- Ackermann, M. et al. 2011b *ApJ*, 741, 30
- Ackermann, M., Ajello, M., Allafort, A. et al. 2012 *ApJ*, 753, 83
- Agudo, I., Thum, C., Gómez, J.L., & Wiesemeyer, H. 2014, *A&A*, 566, 59
- Aharonian F. A., 2000, *New Astronomy*, 5, 377
- Ahn, C. P., Alexandroff, R., Allende Prieto, C. et al. 2012, *ApJS*, 203, 21
- Ajello, M., Gasparrini, D., Sanchez-Conde, M. et al., 2015, *ApJ*, 800, L27
- Becker, R. H., White, R. L., Helfand, D. J. 1995 *ApJ*, 450, 559
- Berlin A., Hooper D., 2014, *Phys. Rev. D*, 89, 016014
- Bianchini, V., Foschini, L., Ghisellini, G., et al. 2009, *A&A* 496, 423
- Blandford, R. D., Rees, M. J., 1978, *PROC. Pittsburgh Conference on BL Lac objects*, 328
- Bonnarel, F., Fernique, P., Bienaymé, O. et al. 2000 *A&AS*, 143, 33
- Cardelli, J. A., Clayton, G. C. & Mathis, J. S. 1989, *ApJ*, 345, 245
- Cohen, A. S., Lane, W. M., Cotton, W. D. et al. 2007 *AJ*, 134, 1245
- Condon, J. J., Cotton, W. D., Greisen, E. W. et al. 1998, *AJ*, 115, 1693
- Cutri et al. 2012 *wiserept*, 1C
- D'Abrusco, R., Massaro, F., Ajello, M., Grindlay, J. E., Smith, Howard A. & Tosti, G. 2012 *ApJ*, 748, 68
- D'Abrusco, R., Massaro, F., Paggi, A. et al. 2013 *ApJS*, 206, 12
- D'Abrusco, R., Massaro, F., Paggi, A., Smith, H. A., Masetti, N., Landoni, M., & Tosti, G. 2014, *ApJS*, 215, 14
- D'Abrusco, R. et al. 2016 *ApJS* in prep.
- Doert, M. & Errando, M. 2014 *ApJ*, 782, 41
- Douglas, J. N., Bash, F. N., Bozayan, F. A., Torrence, G. W., Wolfe, C. 1996 *AJ*, 111, 1945
- Evans, I. N., Primini, F. A., Glotfelty, K. J. et al. 2010 *ApJS*, 189, 37
- Evans, P. A., Osborne, J. P., Beardmore, A. P. et al. 2014 *ApJS*, 210, 8
- Falco, E. E., Kochanek, C. S., Munoz, J. A., 1998, *ApJ*, 494, 47
- Falomo, R., Pian, E., & Treves, A. 2014, *A&ARv*, 22, 73
- Ghisellini G., Tavecchio F., Foschini L., Sbaratto T., Ghirlanda G., Maraschi L., 2012, *MNRAS*, 425, 1371
- Giommi P., Padovani P., 1994, *MNRAS*, 268, L51
- Giommi P., Padovani P., Polenta G., Turriziani S., D'Élia V., Piranomonte S., 2012, *MNRAS*, 420, 2899
- Giommi, P., Padovani, P., & Polenta, G. 2013, *MNRAS*, 431, 1914
- Gregory, P. C. & Condon, J. J. 1991 *ApJS*, 75, 1011
- Gregory, P. C., Scott, W. K., Douglas, K., Condon, J. J. 1996 *ApJS*, 103, 427
- Hassan, T., Mirabal, N., Contreras, J. L., Oya, I. 2013 *MNRAS*, 428, 220
- Homan, D. C., Ojha, R., Wardle, J. F. C., Roberts, D. H., Aller, M. F., Aller, H. D., & Hughes, P. A. 2002, *ApJ*, 568, 99
- Horne, K. 1986, *PASP*, 98, 609
- Hovatta, T., Lister, M. L., Aller, M. F., et al. 2012, *AJ*, 144, 105
- Hovatta, T., Aller, M. F., Aller, H. D., et al. 2014, *AJ*, 147, 143
- Inoue, S., & Takahara, F. 1996, *ApJ*, 463, 555
- Jones H. D. et al. 2009 *MNRAS*, 399, 683
- Jones, D. H., Saunders, W., Colless, M., et al. 2004, *MNRAS*, 355, 747
- Kellermann, K. I., Lister, M. L., Homan, D. C., Ros, E., Zensus, J. A., Cohen, M. H., Russo, M., & Vermeulen, R. C. 2003, *High Energy Blazar Astron.*, 299, 117
- Kovalev, Y. Y. 2009, *ApJL*, 707, L56
- Landoni, M.; Falomo, R.; Treves, A.; Sbarufatti, B.; Barattini, M.; Decarli, R.; Kotilainen, J. 2013 *AJ*, 145, 114
- Landoni, M., Massaro, F. et al. 2015 *AJ*, 149, 63
- Landt H., Padovani P., Giommi P., 2002, *MNRAS*, 336, 945
- Lane, W. M., Cotton, W. D., van Velzen, S. et al. 2014 *MNRAS*, 440, 327
- Laurent-Muehleisen, S.A. et al., 1999, *ApJ*, 525, 127
- Lister, M. L., Aller, H. D., Aller, M. F. et al. 2009a, *AJ*, 137, 3718
- Marscher A. P. et al., 2010, *ApJ*, 710, L126
- Massaro, E., Giommi, P., Leto, C. et al. 2009 *A&A*, 495, 691
- Massaro, F., D'Abrusco, R., Ajello, M., Grindlay, J. E. & Smith, H. A. 2011a *ApJ*, 740L, 48
- Massaro, E., Giommi, P., Leto, C. et al. 2011b "Multifrequency Catalogue of Blazars (3rd Edition)", ARACNE Editrice, Rome, Italy
- Massaro, F., D'Abrusco, R., Tosti, G., Ajello, M., Paggi, A., Gasparrini, 2012a *ApJ*, 752, 61
- Massaro, F., D'Abrusco, R., Tosti, G., Ajello, M., Gasparrini, D., Grindlay, J. E. & Smith, Howard A. 2012b *ApJ*, 750, 138
- Massaro, F., D'Abrusco, R., Paggi, A., Tosti, G., Gasparrini, D. 2012c *ApJ*, 750L, 35
- Massaro, E., Nesci, R., Piranomonte, S. et al. 2012d *MNRAS*, 422, 2322
- Massaro, F., D'Abrusco, R., Paggi, A. et al. 2013a *ApJS*, 206, 13
- Massaro, F., D'Abrusco, R., Giroletti, M. et al. 2013b *ApJS*, 207, 4
- Massaro, F., Masetti, N., D'Abrusco, R. et al. 2014a *AJ*, 148, 66
- Massaro, F., Giroletti, M., D'Abrusco, R. et al. 2014b *ApJS*, 213, 3
- Massaro, E., Maselli, A., Leto, C. et al.: "Multifrequency Catalogue of blazars 5th Edition", Aracne, Roma (2015)
- Massaro, F., D'Abrusco, R., Landoni, M. et al. 2015b, *ApJS*, 217, 2
- Massaro, F., Landoni, M., D'Abrusco, R. et al. 2015c, *A&A*, 575, 124
- Masetti, N., Sbarufatti, B., Parisi, P. 2013 *A&A*, 559A, 58
- Mirabal, N., Frias-Martinez, V., Hassan, T., & Frias-Martinez, E. 2012, *MNRAS*, 424, 64
- Murphy, T. et al. 2010 *MNRAS*, 402, 2403
- Nolan, P. L., Abdo, A. A., Ackermann, M. et al. 2012 *ApJS*, 199, 31
- Nori, M., Giroletti, M., Massaro, F., D'Abrusco, R., Paggi, A. & Tosti, G. et al. 2014 *ApJS* 212, 3
- Padovani P., Giommi P., 1995, *MNRAS*, 277, 1477
- Paggi, A., Massaro, F., D'Abrusco, R. et al. 2013 *ApJS*, 209, 9
- Paggi, A., Milisavljevic, D., Masetti, N. et al. 2014 *AJ*, 147, 112
- Petrov, L., Mahony, E. K., Edwards, P. G. et al. 2013 *MNRAS*, 432, 1294
- Rengelink, R., Tang, Y., de Bruyn, A. G. et al. 1997, *A&A Suppl.* 124, 259
- Saxton, R.D. 2008 *A&A*, 480, 611
- Ricci F, Massaro F., Landoni M., D'Abrusco R., Milisavljevic D., Stern D., Masetti N., Paggi A., Smith Howard A. & Tosti G. 2015, *AJ*, 149, 160
- Seibert, M. 2012 "Galaxy Evolution Explorer (GALEX) Medium-deep Sky Catalog based on GALEX General Release 6"
- Schinzl, F., Cutchin, S. E., Polisenky, E., Helmboldt, J. F., Dowell, J.; Kassim, N. E., Taylor, G. B., 2014, *AAS Meeting #223*, #148.22
- Schlegel, D. J., Finkbeiner, D. P. & Davis, M. 1998, *ApJ*, 500, 525
- Shaw, M. S., Romani, R. W.; Cotter, G. et al. 2013 *ApJ*, 764, 135
- Shaw, M. S., Filippenko, A. V., Romani, R. W. et al. 2013 *AJ*, 146, 127
- Stern, D. & Assef, R. J. 2013 *ApJ*, 764L, 30
- Skrutskie, M. F. et al. 2006, *AJ*, 131, 1163
- Stickel, M. et al. 1991 *ApJ*, 374, 431
- Stoeckel et al. 1991, *ApJS*, 76, 813
- Stroh, M. C. & Falcone, A. D. 2013, *ApJS*, 207, 28
- Takeuchi, Y., Kataoka, J., Maeda, K. et al. 2013 *ApJS*, 208, 25
- Taylor, M. B. 2005, *ASP Conf. Ser.*, 347, 29
- Taylor, G. B., Healey, S. E., Helmboldt, J. F., et al. 2007, *ApJ*, 671, 1355
- Today, D. 1986 *SPIE*, 627, 733
- Urry, C. M., & Padovani, P. 1995, *PASP*, 107, 803
- Vermeulen, R.C., & Cohen, M.H., 1994, *ApJ*, 430
- Vermeulen R. C., et al., 1995, *ApJ*, 452, L5
- Voges, W. et al. 1999 *A&A*, 349, 389
- Voges, W. et al. 2000 *IAUC*, 7432R, 1.
- Warwick, R. S., Saxton, R. D., Read, A. M. 2012, *A&A*, 548A, 99
- White, R. L., Becker, R. H. Helfand, D. J., Gregg, M. D. et al. 1997 *ApJ*, 475, 479
- White, R. L., Becker, R. H., Gregg, M. D., et al. 2000, *ApJS*, 126, 133
- Wright, A. & Otrupcek, R. 1990 *PKS*, C, 0
- Wright, A. E., Griffith, M.R., Burke, B.F., Ekers, R.D. 1994 *ApJS*, 91, 111
- Wright, E. L., et al. 2010 *AJ*, 140, 1868